

# Logarithmic Minimal Models with Robin Boundary Conditions

Jean-Emile Bourgine<sup>†</sup>, Paul A. Pearce<sup>\*</sup>, Elena Tartaglia<sup>\*</sup>

<sup>†</sup>*INFN Bologna, Università di Bologna  
Via Irnerio 46, 40126 Bologna, Italy  
on leave from*

*Asia Pacific Center for Theoretical Physics (APCTP)  
Pohang, Gyeongbuk 790-784, Republic of Korea*

<sup>\*</sup>*School of Mathematics and Statistics, University of Melbourne  
Parkville, Victoria 3010, Australia*

bourgine@bo.infn.it, p.pearce@ms.unimelb.edu.au, elena.tartaglia@unimelb.edu.au

## Abstract

We consider general logarithmic minimal models  $\mathcal{LM}(p, p')$ , with  $p, p'$  coprime, on a strip of  $N$  columns with the  $(r, s)$  Robin boundary conditions introduced by Pearce, Rasmussen and Tipunin. On the lattice, these models are Yang-Baxter integrable loop models that are described algebraically by the one-boundary Temperley-Lieb algebra. The  $(r, s)$  Robin boundary conditions are a class of integrable boundary conditions satisfying the boundary Yang-Baxter equations which allow loop segments to either reflect or terminate on the boundary. The associated conformal boundary conditions are organized into infinitely extended Kac tables labelled by the Kac labels  $r \in \mathbb{Z}$  and  $s \in \mathbb{N}$ . The Robin vacuum boundary condition, labelled by  $(r, s - \frac{1}{2}) = (0, \frac{1}{2})$ , is given as a linear combination of Neumann and Dirichlet boundary conditions. The general  $(r, s)$  Robin boundary conditions are constructed, using fusion, by acting on the Robin vacuum boundary with an  $(r, s)$ -type seam consisting of an  $r$ -type seam of width  $w$  columns and an  $s$ -type seam of width  $d = s - 1$  columns. The  $r$ -type seam admits an arbitrary boundary field which we fix to the special value  $\xi = -\frac{\lambda}{2}$  where  $\lambda = \frac{(p' - p)\pi}{2p'}$  is the crossing parameter. The  $s$ -type boundary introduces  $d$  defects into the bulk. We consider the commuting double-row transfer matrices and their associated quantum Hamiltonians and calculate analytically the boundary free energies of the  $(r, s)$  Robin boundary conditions. Using finite-size corrections and sequence extrapolation out to system sizes  $N + w + d \leq 26$ , the conformal spectrum of boundary operators is accessible by numerical diagonalization of the Hamiltonians. Fixing the parity of  $N$  for  $r \neq 0$  and restricting to the ground state sequences  $w = \lfloor \frac{|r|p'}{p} \rfloor$ ,  $r \in \mathbb{Z}$  with the inverse  $r = (-1)^{N+w+d} \lceil \frac{pw}{p'} \rceil$ , we find that the conformal weights take the values  $\Delta_{r, s - \frac{1}{2}}^{p, p'}$  where  $\Delta_{r, s}^{p, p'}$  is given by the usual Kac formula. The  $(r, s)$  Robin boundary conditions are thus conjugate to scaling operators with half-integer values for the Kac label  $s - \frac{1}{2}$ . Level degeneracies support the conjecture that the characters of the associated (reducible or irreducible) representations are given by Virasoro Verma characters.

**Keywords:** Exactly solvable models, logarithmic conformal field theory, loop models

# Contents

<b>1</b>	<b>Introduction</b>	<b>3</b>
<b>2</b>	<b>Logarithmic Minimal Models and Robin Boundary Conditions</b>	<b>4</b>
2.1	Temperley-Lieb algebra and local relations . . . . .	4
2.2	Robin link states . . . . .	5
2.3	One-boundary Temperley-Lieb algebra . . . . .	6
2.4	Robin vacuum boundary condition . . . . .	7
2.5	Integrable $(r, s)$ Robin boundary conditions . . . . .	8
<b>3</b>	<b>Transfer Matrices, Hamiltonians and Non-Universal Quantities</b>	<b>10</b>
3.1	Commuting double-row transfer matrices . . . . .	10
3.2	Quantum Hamiltonians . . . . .	10
3.3	Bulk and boundary free energies . . . . .	11
<b>4</b>	<b>Finite-Size Spectra</b>	<b>14</b>
4.1	Finitized characters . . . . .	14
4.2	Logarithmic limit . . . . .	17
4.3	Finite-size corrections . . . . .	18
4.4	Numerical conformal weights . . . . .	19
4.5	Numerical conformal partition functions . . . . .	22
<b>5</b>	<b>Conclusion</b>	<b>25</b>
<b>A</b>	<b>Derivation of the Inversion Relation</b>	<b>26</b>
A.1	Inversion relation for the Robin vacuum boundary . . . . .	26
A.2	Inversion relation for a Robin boundary with an $r$ -type seam . . . . .	27
<b>B</b>	<b>Solution of the Inversion Relation</b>	<b>28</b>
B.1	Solution of the inversion relation for the Robin vacuum . . . . .	28
B.2	Solution of the inversion relation with an $r$ -type seam . . . . .	29
<b>C</b>	<b>Boundary Algebra</b>	<b>30</b>
C.1	Robin boundaries as representations of one-boundary TL algebra . . . . .	30
C.2	Algebraic equivalence of Robin boundary conditions . . . . .	31

# 1 Introduction

It is well established that, in the continuum scaling limit, Conformal Field Theories (CFTs) such as the family of minimal models  $\mathcal{M}(m, m')$  [1] describe the universal scaling properties of two-dimensional lattice models. In the case of unitary [2] minimal models,  $m = m' - 1$ , the associated lattice models are the multicritical Ising models [3]. The simplest CFTs fall into the class of rational CFTs [4, 5] which are characterized by a finite number of primary scaling operators. The representations associated with these operators are irreducible and close among themselves under fusion. For rational boundary CFTs [6], the conformal boundary conditions are conjugate (in one-to-one correspondence) to the primary scaling operators. It follows that the conformal data, including the central charges and conformal weights, can be obtained from the lattice by studying the finite-size corrections [7, 8] to the eigenvalues of the transfer matrices, or equivalently, the associated one-dimensional quantum Hamiltonians.

In fact, many CFTs are realized as the continuum scaling limit of Yang-Baxter integrable lattice models [9]. For example, the minimal models describe the continuum scaling limit of the Restricted Solid-On-Solid (RSOS) lattice models [10]. A boundary condition on the lattice is integrable if it satisfies the boundary Yang-Baxter equation [11–13]. Invariably, if a rational CFT is associated with a lattice model that is Yang-Baxter integrable in the bulk, it seems possible to construct a representative integrable lattice boundary condition to realize each of the conformal boundary conditions in the continuum scaling limit. This program has been carried to completion [14] for the critical  $A$ - $D$ - $E$  RSOS models [15] associated with the  $A$ - $D$ - $E$  minimal models [16]. The RSOS models have degrees of freedom in the form of local heights. The continuum scaling limit of such theories with local degrees of freedom are described by rational CFTs.

In this paper, we study the logarithmic minimal models  $\mathcal{LM}(p, p')$  [17] with Virasoro conformal symmetry (as opposed to  $\mathcal{W}$ -extended conformal symmetry [18]). The first members of this family are critical dense polymers  $\mathcal{LM}(1, 2)$  [19] and the loop version  $\mathcal{LM}(2, 3)$  [20] of the square lattice bond percolation model. Like the minimal models [21], the logarithmic minimal models are coset CFTs [22, 23]. But unlike the minimal models, these theories describe systems with nonlocal degrees of freedom in the form of loop segments. The continuum scaling limit of such theories with nonlocal degrees of freedom are described by logarithmic CFTs [24] that are nonunitary and non-rational. The family of logarithmic minimal models plays the same role for logarithmic CFTs that the minimal models play for rational CFTs. The properties of logarithmic CFTs, however, are profoundly different to those of rational CFTs. Most importantly, these theories are characterized [25] by the existence of reducible yet indecomposable representations but, as yet, there is no exhaustive classification of all possible representations. Instead, the focus has been on identifying different kinds of Virasoro representations such as irreducible, fully reducible, projective and their  $\mathcal{W}$ -algebra counterparts. In the logarithmic context, it is no longer true in general that each representation is conjugate to a conformal boundary condition. For the logarithmic minimal models, however, it is known [17, 26–29] that there are a countably infinite number of Virasoro Kac representations with conjugate  $(r, s)$  boundary conditions organized into infinitely extended Kac tables. The central charges and conformal weights, given by the Kac formula, are

$$c = c^{p,p'} = 1 - \frac{6(p' - p)^2}{pp'}, \quad \Delta_{r,s}^{p,p'} = \frac{(rp' - sp)^2 - (p' - p)^2}{4pp'}, \quad 1 \leq p < p', \quad r, s \in \mathbb{N} \quad (1.1)$$

All of these models are nonunitary with effective central charge  $c_{\text{eff}} = 1$ .

The conformal properties of polymers and percolation have been studied [30–33] since the late eighties. Remarkably, there are indications [31, 33] that certain representations occur with conformal weights given by the Kac formula (1.1) with half-integer Kac labels. Indeed, it has been suggested [34] that a field with conformal weight  $\Delta_{2, \frac{5}{2}}^{2,3} = 0$  plays the role of Watts' [35] primary field in the description

of critical percolation. Moreover, the existence of a family of spin fields with conformal weights  $\Delta_{r-\frac{1}{2},0}^{p,p+1}$  for  $r \in \mathbb{N}$  has recently been posited [36]. We restrict  $r$  and  $s$  to be integers and use  $r, s$  as integer Kac labels and  $r - \frac{1}{2}, s - \frac{1}{2}$  as half-integer Kac labels throughout this paper.

Robin boundary conditions [37] are linear combinations of Neumann and Dirichlet boundary conditions. In the context of loop models, they allow loop segments to either reflect or terminate at the boundary. In this paper, we apply the  $(r, s)$  Robin boundary conditions of Pearce, Rasmussen and Tipunin [38] to the general minimal models and confirm numerically that the associated conformal weights are  $\Delta_{r,s-\frac{1}{2}}^{p,p'}$  where  $r \in \mathbb{Z}$  and  $s \in \mathbb{N}$ . The  $(r, s)$  Robin boundary conditions are thus conjugate to scaling operators with half-integer values for the Kac label  $s - \frac{1}{2}$ . In particular, the Robin vacuum  $(r, s - \frac{1}{2}) = (0, \frac{1}{2})$  has conformal weight

$$\Delta_{0,\frac{1}{2}}^{p,p'} = -\frac{(2p' - p)(2p' - 3p)}{16pp'}, \quad 1 \leq p < p', \quad p, p' \in \mathbb{N} \quad (1.2)$$

These results were established analytically in [38] for critical dense polymers  $\mathcal{LM}(1, 2)$  with  $\beta = 0$ . The  $(r, s)$  Robin boundary conditions are so-named because of the  $(r, s)$ -type seam by which they are constructed. The  $(r, s)$  Robin boundary conditions have similarities to the so-called JS boundary conditions [39]. The main differences are that the  $(r, s)$  Robin boundary conditions are (i) manifestly Yang-Baxter integrable and (ii) they are constructed using standard  $r$ - and  $s$ -type seams, which behave as topological defects. These seams propagate freely along the row due to the generalized Yang-Baxter equation and ensure the expected  $su(2)$  fusion rules for Cardy fusion [40] of boundary conditions on the lattice.

The layout of this paper is as follows. In Section 2, we describe the logarithmic minimal lattice models on the strip in terms of the one-boundary Temperley-Lieb algebra. Following [38], we recall the definition of the Robin link states and the construction of the integrable  $(r, s)$  Robin boundary conditions. The commuting double-row transfer matrices and their associated quantum Hamiltonians are revisited in Section 3. The analytic derivation of the exact bulk and boundary free energies and their Hamiltonian limits are also given in this section. The details of the derivation and solution of the inversion relation are relegated to Appendices A and B. Our numerical results for the finite-size spectra are presented in Section 4 along with a discussion of the finitized conformal partition functions and the logarithmic limit. Properties of the Robin boundaries as representations of the one-boundary Temperley-Lieb algebra are discussed in Appendix C. Some final remarks are given in the conclusion.

## 2 Logarithmic Minimal Models and Robin Boundary Conditions

### 2.1 Temperley-Lieb algebra and local relations

We study the logarithmic minimal models  $\mathcal{LM}(p, p')$  [17] on a square lattice with the geometry of the strip and apply Robin boundary conditions. Here  $p, p'$  are coprime integers with  $1 \leq p < p'$ . The models are built using the one-boundary Temperley-Lieb (TL) or blob algebra [20, 41–45] and describe the statistical interaction of densely packed self- and mutually-avoiding loops. The strip has  $N$  bulk columns and  $2M$  rows and is built by  $M$  applications of the double-row transfer matrix. Closed loops in the bulk have a fugacity  $\beta = 2 \cos \lambda$  where the crossing parameter is

$$\lambda = \frac{(p' - p)\pi}{p'}, \quad 1 \leq p < p', \quad p, p' \in \mathbb{N} \quad (2.1)$$

Loop configurations on the square lattice are built on two face tiles which are the generators of

the planar TL algebra [46]

$$\begin{array}{|c|} \hline \text{[Square with two arcs from bottom-left to top-right]} \\ \hline \end{array} \quad \text{and} \quad \begin{array}{|c|} \hline \text{[Square with two arcs from top-left to bottom-right]} \\ \hline \end{array} \quad (2.2)$$

These tiles, corresponding to the identity  $I$  and monoids  $e_j$  respectively, can be viewed as operators acting from the bottom-left edges to the top-right edges of an elementary face. Together they generate the linear TL algebra

$$TL_N(\beta) := \langle I, e_j; j = 1, \dots, N-1 \rangle \quad (2.3)$$

satisfying the relations

$$e_j e_{j\pm 1} e_j = e_j, \quad e_j^2 = \beta e_j, \quad e_j e_k = e_k e_j, \quad |j - k| \geq 2 \quad (2.4)$$

The diagrammatic action of the tiles on a set of  $N$  parallel strings, where  $e_j$  acts between string  $j$  and  $j+1$ , gives a faithful representation of the algebra

$$I = \begin{array}{|c|} \hline \text{[Vertical lines 1, 2, \dots, N-1, N]} \\ \hline \end{array} \quad e_j = \begin{array}{|c|} \hline \text{[Vertical lines 1, 2, \dots, j, j+1, \dots, N-1, N with arcs between j and j+1]} \\ \hline \end{array} \quad (2.5)$$

To build commuting transfer matrices [17], we introduce a spectral parameter  $u$  related to spatial anisotropy [47]. Face operators are defined as the linear combinations

$$\begin{array}{|c|} \hline \text{[Square with marked corner and parameter u]} \\ \hline \end{array} := s_1(-u) \begin{array}{|c|} \hline \text{[Square with two arcs from bottom-left to top-right]} \\ \hline \end{array} + s_0(u) \begin{array}{|c|} \hline \text{[Square with two arcs from top-left to bottom-right]} \\ \hline \end{array}, \quad X_j(u) = s_1(-u)I + s_0(u)e_j \quad (2.6)$$

where

$$s(u) = s_0(u), \quad s_k(u) := \frac{\sin(u + k\lambda)}{\sin \lambda}, \quad k \in \mathbb{Z} \quad (2.7)$$

and the marked corner fixes the orientation of the face. The face operators satisfy the Yang-Baxter equation

$$X_{j+1}(u)X_j(u+v)X_{j+1}(v) = X_j(v)X_{j+1}(u+v)X_j(u) \quad (2.8)$$

or diagrammatically

$$\begin{array}{|c|} \hline \text{[Hexagon with parameters v, v-u, u]} \\ \hline \end{array} = \begin{array}{|c|} \hline \text{[Hexagon with parameters v-u, u, v]} \\ \hline \end{array} \quad (2.9)$$

The face operators  $X_j$  also satisfy the local inversion and crossing relations

$$\begin{array}{|c|} \hline \text{[Two diamonds with parameters u, -u]} \\ \hline \end{array} = s(\lambda - u)s(\lambda + u) \begin{array}{|c|} \hline \text{[Diamond with two arcs]} \\ \hline \end{array}, \quad \begin{array}{|c|} \hline \text{[Square with parameter u]} \\ \hline \end{array} = \begin{array}{|c|} \hline \text{[Square with parameter \lambda - u]} \\ \hline \end{array} \quad (2.10)$$

## 2.2 Robin link states

In this section we describe the link states associated with  $(r, s)$  Robin boundary conditions. We denote the vector space of Robin link states by  $\mathcal{V}_d^{(N, w)}$ . A link state on  $N$  bulk and  $w$  boundary nodes is a planar diagram of non-crossing arc segments. It contains  $d = s - 1 \geq 0$  defects (vertical line segments) attaching individual nodes to a point above at infinity and  $b \geq 0$  boundary links linking individual nodes to the right boundary. The remaining  $\frac{1}{2}(N + w - d - b)$  nodes are connected pairwise by half-arcs with

$$w = \text{width of } r\text{-type seam}, \quad N + w - d - b = 0 \pmod{2} \quad (2.11)$$

A Robin link state satisfies the three properties:

- (i) no half-arc joins a pair of boundary nodes
- (ii) no boundary link emanates from a boundary node
- (iii) every boundary node is either a defect or is linked to a bulk node

In the Robin vacuum sector with  $w = d = 0$ , the vector space of link states with  $N = 4$  is

$$\mathcal{V}_0^{(4,0)} = \text{span} \left\{ \begin{array}{c} \text{---} \text{---} \text{---} \text{---} \\ \text{---} \text{---} \text{---} \text{---} \\ \text{---} \text{---} \text{---} \text{---} \\ \text{---} \text{---} \text{---} \text{---} \\ \text{---} \text{---} \text{---} \text{---} \\ \text{---} \text{---} \text{---} \text{---} \end{array} \right\} \quad (2.12)$$

The number of these link states is  $\dim \mathcal{V}_0^{(N,0)} = \binom{N}{\lfloor N/2 \rfloor}$ . Examples of vector spaces of Robin link states with defects are

$$\begin{aligned} \mathcal{V}_1^{(3,1)} &= \text{span} \left\{ \begin{array}{c} | \text{---} \text{---} \text{---} \\ | \text{---} \text{---} \text{---} \\ | \text{---} \text{---} \text{---} \end{array} \right\} \\ \mathcal{V}_1^{(3,2)} &= \text{span} \left\{ \begin{array}{c} | \text{---} \text{---} \text{---} \\ | \text{---} \text{---} \text{---} \\ | \text{---} \text{---} \text{---} \end{array} \right\} \\ \mathcal{V}_0^{(4,2)} &= \text{span} \left\{ \begin{array}{c} \text{---} \text{---} \text{---} \text{---} \\ \text{---} \text{---} \text{---} \text{---} \\ \text{---} \text{---} \text{---} \text{---} \\ \text{---} \text{---} \text{---} \text{---} \end{array} \right\} \end{aligned} \quad (2.13)$$

where the dashed line separates the bulk and right boundary. The number of these link states is

$$\dim \mathcal{V}_d^{(N,w)} = \binom{N}{\lfloor \frac{N-d}{2} \rfloor + (-1)^{N-d-w} \lceil \frac{w}{2} \rceil} \quad (2.14)$$

The defects can be closed to an  $s$ -type seam on the left or, equivalently, on the right by passing under the boundary links. The latter is used in the construction of Robin boundaries using  $(r, s)$ -type seams but the former implementation is convenient in our numerical calculations. The dimension of the vector space  $\mathcal{V}^{(N,w)}$  of Robin link states with an arbitrary number of defects is *independent* of  $w$

$$\dim \mathcal{V}^{(N,w)} = \sum_{d=0}^{N+w} \dim \mathcal{V}_d^{(N,w)} = 2^N \quad (2.15)$$

### 2.3 One-boundary Temperley-Lieb algebra

The one-boundary TL or blob algebra [41–45] is a planar diagrammatic algebra generated by two bulk face tiles and one boundary triangle

$$\begin{array}{c} \square \quad \square \quad \triangle \\ \text{---} \quad \text{---} \quad \text{---} \end{array} \quad (2.16)$$

Fixing the direction of transfer gives the linear one-boundary TL algebra

$$TL_N(\beta; \beta_1, \beta_2) := \langle I, e_j, f_N; j = 1, \dots, N-1 \rangle \quad (2.17)$$

where  $\beta_1, \beta_2$  are fugacities of loops that terminate on the boundary. The generators

$$I := \begin{array}{c} | \quad | \quad | \quad \dots \quad | \\ 1 \quad \quad \quad \quad N \end{array}, \quad e_j := \begin{array}{c} | \quad \dots \quad | \quad \text{---} \quad | \quad \dots \quad | \\ 1 \quad \quad \quad j \quad \quad \quad N \end{array}, \quad f_N := \begin{array}{c} | \quad | \quad | \quad \dots \quad | \quad \text{---} \\ 1 \quad \quad \quad \quad \quad \quad N \end{array} \quad (2.18)$$

satisfy



which disallows boundary links emanating from the lower edge of the  $r$ -type seam to propagate up to the upper edge. This relation, reflecting a coupling between the Robin vacuum and the  $r$ -type seam, fixes the coincidence of the boundary field  $\xi$  in the  $r$ -type seam and the Robin vacuum. It is convenient to parameterize the boundary loop fugacities by the variables  $R \in \mathbb{R}^+$  and  $\alpha \in [0, 2\pi)$  as

$$\beta_1 = \frac{R \sin \alpha}{\sin \lambda}, \quad \beta_2 = \frac{R \sin(\alpha - \lambda)}{\sin \lambda} \quad (2.25)$$

so that  $\Gamma(u)$  takes a factorized form

$$\Gamma(u) = \Gamma(u|\xi, \alpha) = R s_1(\xi - u) s_0(\xi + u + \alpha) \quad (2.26)$$

This form of  $\Gamma(u)$  and (2.22) agree with (3.46) of [14] with  $\xi_{\text{BP}} = \xi + \lambda$  and  $\alpha = r\lambda$  so that our later specialization to  $\xi = -\frac{\lambda}{2}$ , for the numerics, coincides with the specialization  $\xi_{\text{BP}} = \frac{\lambda}{2}$ . For the numerics, we also specialize to the case  $\beta_1 = \beta_2 = 1$ , for which  $R = 2 \sin \frac{\lambda}{2}$  and

$$\alpha = \frac{\lambda + \pi}{2}, \quad \Gamma(u) = \frac{\sin(\xi + \lambda - u) \cos(\xi + \frac{\lambda}{2} + u)}{\sin \lambda \cos \frac{\lambda}{2}} \quad (2.27)$$

For later reference, in the case  $\beta_1 = \beta_2 = 1$ , we note that

$$\frac{\Gamma(0)}{s_1(\xi)} = s_1(\xi) - s_0(\xi) = \frac{\cos(\xi + \frac{\lambda}{2})}{\cos \frac{\lambda}{2}} \quad (2.28)$$

In the notation of Doikou and Martin [48],  $\mu_{\text{DM}} = \lambda$ ,  $\theta_{\text{DM}} = -iu/\lambda$ ,  $m_{\text{DM}}\lambda = \lambda - \alpha$  and  $\zeta_{\text{DM}}\lambda = \xi + (\lambda + \alpha)/2$  with  $R = 1$ .

At first sight, the Robin boundary conditions depend on the three parameters  $R$ ,  $\xi$  and  $\alpha$  (in addition to the bulk parameters  $u, \lambda$ ). Upon renormalization of the boundary operator  $f_N$ , it can be shown that the parameter  $R \neq 0$  corresponds to an overall scale factor. Let us introduce the quantities  $\tilde{\beta}_1, \tilde{\beta}_2$  independent of  $R$  as  $\beta_1 = R\tilde{\beta}_1$  and  $\beta_2 = R\tilde{\beta}_2$  and define the operator  $\tilde{f}_N$  as  $f_N = R\tilde{f}_N$  such that  $e_{N-1}\tilde{f}_N e_{N-1} = \tilde{\beta}_1 e_{N-1}$  and  $\tilde{f}_N^2 = \tilde{\beta}_2 \tilde{f}_N$ . Noticing that  $\tilde{\Gamma}(u) = R^{-1}\Gamma(u)$  is independent of  $R$ , we deduce that the  $R$ -dependence of the Robin vacuum factorizes

$$\Gamma(u)I + s_0(2u)f_N = R[\tilde{\Gamma}(u)I + s_0(2u)\tilde{f}_N] \quad (2.29)$$

We deduce that the thermodynamic and conformal properties are independent of  $R$  and only depend on the angle  $\alpha$  or, equivalently, on the ratio  $\beta_1/\beta_2$  for  $\beta_2 \neq 0$ .

## 2.5 Integrable $(r, s)$ Robin boundary conditions

Following [14, 17, 38], we dress the Robin vacuum boundary condition by fusing with  $r$ - and  $s$ -type seams on the right boundary

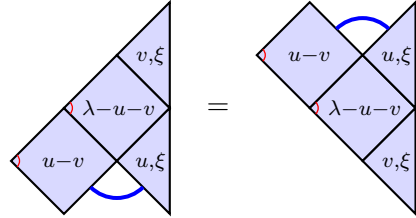
$$(r, s - \frac{1}{2}) = \text{[Diagram]} \quad (2.30)$$



The fusion within a seam is implemented diagrammatically [27,28,49] (as opposed to using Wenzl-Jones projectors) by forbidding closed half-arcs along the lower edge. A drop-down property ensures that no closed half-arcs can occur along the top edge. With the parameters appropriately tuned (2.24) to give a drop-down property of boundary arcs, this gives the general integrable  $(r, s)$  Robin boundary conditions. The column inhomogeneities are  $\xi_k = \xi + k\lambda$  and the dependence on  $\xi$  in the Robin vacuum is suppressed but is coupled to coincide with the value of  $\xi$  in the  $r$ -type seam. The action of the double-row transfer matrix must map  $\mathcal{V}_d^{(N,w)}$  back to itself. This is implemented by the diagrammatic fusion projection in the  $r$ - and  $s$ -type seams and the drop-down property of boundary arcs. In the  $s$ -type seam, this prevents the closing of two defects to form a closed loop ensuring that the number of defects is conserved and  $s$  or  $d$  is a good quantum number. In the  $r$ -type seam, the action also kills [27] certain words among the boundary TL generators. We also note that, due to the generalized Yang-Baxter equation, the  $r$ - and  $s$ -type boundary seams commute and freely propagate along the row under a similarity transformation that preserves the spectrum. In particular, they obey the fusion rules

$$(r, s - \frac{1}{2}) = (r, 1) \otimes (1, s) \otimes (0, \frac{1}{2}) = (r, s) \otimes (0, \frac{1}{2}) \quad (2.31)$$

Using the fact that the Robin vacuum satisfies the boundary Yang-Baxter equation, and following [13], it follows that the  $(r, s)$  Robin boundary conditions satisfy the boundary Yang-Baxter equation



$$(2.32)$$

where the boundary conditions are represented diagrammatically by the  $u$ - or  $v$ -dependent right boundary triangles. Although we do not do so in this paper, similar integrable boundary conditions can be constructed on the left boundary.

As an operator acting on  $\mathcal{V}^{(N,w)}$ , the boundary operator implementing the  $(r, s)$  Robin boundary condition is

$$K_N^{(w)}(u, \xi) = X_N(u - \xi_w) X_{N+1}(u - \xi_{w-1}) \dots X_{N+w-1}(u - \xi_1) [\Gamma(u) I + s_0(2u) f_{N+w}] \\ X_{N+w-1}(u + \xi_1) X_{N+w-2}(u + \xi_2) \dots X_N(u + \xi_w) \quad (2.33)$$

When restricted to acting from  $\mathcal{V}_d^{(N,w)}$  to itself, the boundary operator reduces [38] to

$$K_N^{(w)}(u, \xi) \simeq \prod_{j=1}^w s_{-1}(u + \xi_j) s_{-1}(u - \xi_j) \left[ \alpha_0^{(w)} I + \alpha_1^{(w)} e_N + \alpha_2^{(w)} e_N e_{N+1} + \dots \right. \\ \left. + \alpha_w^{(w)} e_N e_{N+1} \dots e_{N+w-1} + \alpha_{w+1}^{(w)} e_N e_{N+1} \dots e_{N+w-1} f_{N+w} \right] \quad (2.34)$$

where

$$\alpha_0^{(w)} = \Gamma(u) \\ \alpha_k^{(w)} = \frac{(-1)^k s_0(2u)}{s_0(u + \xi) s_{w+1}(\xi - u)} \left( s_{w-k}(\lambda) \Gamma(u) - \beta_1 s_{w-k+1}(u + \xi) s_1(\xi - u) \right), \quad k = 1, 2, \dots, w \\ \alpha_{w+1}^{(w)} = \frac{(-1)^w s_0(2u) s_1(\xi - u)}{s_{w+1}(\xi - u)} \quad (2.35)$$

All other TL words are killed. The similarity sign  $\simeq$  (instead of an equality sign) indicates that the actions agree only when restricted to the vector space  $\mathcal{V}_d^{(N,w)}$ .

### 3 Transfer Matrices, Hamiltonians and Non-Universal Quantities

#### 3.1 Commuting double-row transfer matrices

In this paper, we study the double row transfer matrix  $\mathbf{D}(u)$  with a Neumann or  $(1, 1)$  Kac boundary condition on the left edge of the strip and an  $(r, s)$  Robin boundary condition (2.30) on the right edge of the strip

$$\mathbf{D}(u) := \frac{1}{\mathcal{N}^{(w)}(u, \xi)} \quad \begin{array}{c} \text{Diagram: A double-row transfer matrix with } N \text{ columns. The top row has entries } \lambda - u, \lambda - u, \dots, \lambda - u. \text{ The bottom row has entries } u, u, \dots, u. \text{ The left boundary is a blue arc with a red dot. The right boundary is a blue arc with a red dot and a label } u, \xi. \text{ Red dots are at the corners of each cell.} \end{array} \quad (3.1)$$

This transfer matrix acts on the link states described in Section 2.2 with the fixed  $d = s - 1$  defects closed to the right, under the boundary arcs, and onto the  $s$ -type seam. Following the diagrammatic arguments of [13], the Yang-Baxter and boundary Yang-Baxter equations (2.9) and (2.32) ensure the commutation of the transfer matrices  $\mathbf{D}(u)$  and  $\mathbf{D}(v)$ . As in [38], it also follows that the transfer matrices are crossing symmetric

$$\mathbf{D}(\lambda - u) = \mathbf{D}(u) \quad (3.2)$$

The double row transfer matrix is normalized by a crossing symmetric factor (c.f. (3.4) of [28])

$$\mathcal{N}^{(w)}(u, \xi) = \begin{cases} (-1)^w \beta \Gamma(0) s(\xi) s(\xi_{w+1}) \prod_{j=1}^{w-1} s(\xi_j + u) s(\xi_{j+1} - u), & w > 0 \\ \beta \Gamma(0) \frac{s(\xi) s(\xi_1)}{s(\xi + u) s(\xi_1 - u)}, & w = 0 \end{cases} \quad (3.3)$$

so that, in addition, it satisfies  $\mathbf{D}(0) = \mathbf{D}(\lambda) = I$ . For  $w \geq 2$ , the product removes the common factors resulting from fusion in the seam, otherwise, this product takes the value 1. Note, by convention [13], the (normalized) weight associated with an  $r$ -type seam of width  $w = 0$  is not unity and is effectively fixed to

$$\tilde{\kappa}_0(u, \xi) = \tilde{\kappa}_0(\lambda - u, \xi) = \frac{s(\xi + u) s(\xi_1 - u)}{s(\xi) s(\xi_1)} \quad (3.4)$$

#### 3.2 Quantum Hamiltonians

In this paper we work with the normalized transfer matrix  $\mathbf{D}(u)$  given in (3.1). But, to take the Hamiltonian limit, it is convenient to use a transfer matrix normalized as in [38]

$$\mathbf{d}(u) = \frac{\mathcal{N}^{(w)}(u, \xi)}{\eta(u)} \mathbf{D}(u), \quad \eta(u) = \frac{\beta \Gamma(0) s(u + \xi_w) s(\xi) \eta^{(w)}(u, \xi)}{s(u + \xi) s(\xi_w)} \quad (3.5)$$

where

$$\eta^{(w)}(u, \xi) = \prod_{j=1}^w s_{-1}(u + \xi_j) s_{-1}(u - \xi_j), \quad \frac{\eta(u)}{\mathcal{N}^{(w)}(u, \xi)} = \frac{s(u + \xi_w) s(\xi_{w+1} - u)}{s(\xi_w) s(\xi_{w+1})} \quad (3.6)$$

With this normalization the transfer matrix  $\mathbf{d}(u)$  is crossing symmetric  $\mathbf{d}(\lambda - u) = \mathbf{d}(u)$  and satisfies the initial condition  $\mathbf{d}(0) = I$ .

The commuting family  $\mathbf{D}(u)$  of double-row transfer matrices produces an infinite set of commuting conserved quantities by expansion in the spectral parameter  $u$ . The Hamiltonian  $\mathcal{H}$  arises as the first non-trivial operator in the limit  $u \rightarrow 0$

$$\mathbf{d}(u) = \frac{\mathcal{N}^{(w)}(u, \xi)}{\eta(u)} \mathbf{D}(u) = I - \frac{2u}{\sin \lambda} (\mathcal{H} + hI) + \mathcal{O}(u^2) \quad (3.7)$$

where  $h$  measures a convenient shift in the groundstate energy. Explicitly, as an operator acting on the vector space  $\mathcal{V}_d^{(N,w)}$  with  $\beta_1 = \beta_2 = 1$  and  $\lambda \neq \frac{\pi}{2}$ , the Hamiltonian is [38]

$$\begin{aligned} \mathcal{H} = \mathcal{H}^{w,d} \simeq & - \sum_{j=1}^{N-1} e_j - \sum_{k=1}^w \frac{(-1)^k}{s_0(\xi) s_{w+1}(\xi)} \left( s_{w-k}(\lambda) - \frac{s_1(\xi) s_{w-k+1}(\xi)}{\Gamma(0)} \right) e_N e_{N+1} \dots e_{N+k-1} \\ & - (-1)^w \frac{s_1(\xi)}{s_{w+1}(\xi) \Gamma(0)} e_N e_{N+1} \dots e_{N+w-1} f_{N+w} \end{aligned} \quad (3.8a)$$

$$= - \sum_{j=1}^{N-1} e_j - \frac{\cos \frac{\lambda}{2}}{s_{w+1}(\xi) \cos(\xi + \frac{\lambda}{2})} \sum_{k=0}^w (-1)^k \frac{\cos((w-k-\frac{1}{2})\lambda)}{\cos \frac{\lambda}{2}} e_N e_{N+1} \dots e_{N+k} \quad (3.8b)$$

$$= - \sum_{j=1}^{N-1} e_j - \frac{\cos \frac{\lambda}{2}}{s_{w+1}(\xi) \cos(\xi + \frac{\lambda}{2})} F_N \quad (3.8c)$$

where, by convention, we set  $e_{N+w} = f_{N+w}$  and  $F_N$  is a generalized projector described in Appendix C.1. We observe that the boundary term is singular at  $\xi + \alpha = 0 \pmod{\pi}$  and at  $\xi + (w+1)\lambda = 0 \pmod{\pi}$ . So it is anticipated that the boundary energies will be discontinuous at these points. Fixing  $\lambda, w$  and varying  $\xi$ , it follows that the singularities occur at one or two points in the interval  $[0, \pi)$ . The two points coincide whenever  $(w + \frac{1}{2})\lambda = \frac{\pi}{2} \pmod{\pi}$ . Allowing for periodicity, the boundary energy  $\mathcal{E}_R(\xi)$  will accordingly consist of one or two analytic branches separated by the points of discontinuity.

Note that  $\mathcal{H}^{w,d}$  is independent of  $d$  which only enters via the vector space of link states on which the Hamiltonian acts. For  $\lambda = \frac{\pi}{2}$ , that is critical dense polymers  $\mathcal{LM}(1, 2)$ , the Hamiltonian is different. In this case, since the  $\mathcal{O}(u)$  term vanishes, the Hamiltonian is given by the  $\mathcal{O}(u^2)$  term in the expansion [38]. In the absence of an  $r$ -type seam ( $w = 0$ ), the Hamiltonian (3.8c) reduces to

$$\mathcal{H} = - \sum_{j=1}^{N-1} e_j - \frac{1}{\Gamma(0)} f_N \quad (3.9)$$

This is the Hamiltonian studied by Jacobsen and Saleur [39]. In this case, they argue that the conformal properties depend on the sign of  $\beta_2/\Gamma(0)$  or, equivalently, the value of the parameter  $\xi \in [0, \pi)$ . The JS critical phase corresponds to

$$0 < \frac{\beta_2}{\Gamma(0)} = \frac{\sin \lambda \sin(\alpha - \lambda)}{\sin(\xi + \lambda) \sin(\xi + \alpha)} \quad (3.10)$$

### 3.3 Bulk and boundary free energies

The logarithmic minimal models  $\mathcal{LM}(p, p')$  [17] are exactly solvable on the lattice. The key to this exact integrability are functional equations in the form of  $T$ - and  $Y$ -systems [50–52, 13]. Indeed, it is known [53] that the logarithmic minimal models satisfy  $T$ - and  $Y$ -systems on the strip and cylinder. Since the structure of these equations is universal [54] in the sense that the same equations hold

independent of the topology and boundary conditions, it is expected that the same equations will also hold for logarithmic minimal models with  $(r, s)$  Robin boundary conditions. In principle, these equations could be solved for the conformal weights using dilogarithm identities [55, 51]. In practice, the required methodologies have not yet been developed so, in this paper, we calculate the conformal weights numerically. In this section, we use an inversion identity [56], which is the first functional equation in the  $T$ -system, to calculate the bulk and boundary free energies exactly. The bulk free energy is obtained using the inversion relation method [57, 58]. The boundary free energies are calculated using the boundary inversion relation methods of [59, 28]. Knowing the bulk and boundary free energies exactly greatly improves the accuracy of the numerically extrapolated estimates for the conformal weights in Section 4.

The transfer matrix  $\mathbf{D}(u)$  (3.1) satisfies an inversion identity [56] of the form

$$\mathbf{D}(u)\mathbf{D}(u + \lambda) = \phi(\lambda + u)\phi(\lambda - u)I + \phi(u)\mathbf{D}^2(u) \quad (3.11)$$

where  $\mathbf{D}^2(u)$  denotes the transfer matrix at fusion level 2. In calculating the bulk and boundary free energies we observe that, in the physical region, the second term can be neglected since it is exponentially small compared to the first term. This yields an inversion relation, derived in Appendix A, for each eigenvalue

$$\begin{aligned} D(u)D(u + \lambda) &= D(u)D(-u) = \phi(\lambda + u)\phi(\lambda - u) \\ &= [s_1(u)s_1(-u)]^{2N} \frac{s_2(2u)s_2(-2u)}{s_1(2u)s_1(-2u)} \frac{\Gamma(u)\Gamma(-u)}{\beta^2 \Gamma(0)^2} \frac{s(\xi + u)s(\xi - u)s(\xi_{w+1} + u)s(\xi_{w+1} - u)}{s(\xi)^2 s(\xi_{w+1})^2} \end{aligned} \quad (3.12)$$

The inversion relation is sufficient to determine analytically the bulk and boundary free energies in the thermodynamic limit  $N \rightarrow \infty$ . Subsequently, taking the Hamiltonian limit  $u \rightarrow 0$ , yields the exact bulk and boundary energies.

The partition function per site  $\kappa(u, \xi)$ , given by the largest eigenvalue  $D(u)$  of the transfer matrix  $\mathbf{D}(u)$  in a given  $(r, s)$  sector, factorizes into contributions of order  $\mathcal{O}(N)$ ,  $\mathcal{O}(1)$  and  $\mathcal{O}(1/N)$

$$\frac{D(u)}{\tilde{\kappa}_0(u, \xi)} = \kappa(u, \xi) = \kappa_{\text{bulk}}(u)^{2N} \kappa_0(u) \kappa_R(u, w, \xi) \ell(u), \quad \kappa_R(u, w, \xi) = \kappa_R(u, \xi) \kappa_w(u, \xi) \quad (3.13)$$

The non-universal contributions, common to all eigenvalues in the given sector, are denoted by  $\kappa_{\text{bulk}}(u)$ ,  $\kappa_0(u)$ ,  $\kappa_R(u, \xi)$ ,  $\kappa_w(u, \xi)$  and  $\tilde{\kappa}_0(u, \xi)$  for the bulk, the left Kac vacuum, the right Robin vacuum, the  $r$ -type seam of width  $w > 0$  and the zero width seam respectively. They will be determined exactly by solving the inversion relation (3.12). In the case  $w = 0$ , the trivial extra normalization of the transfer matrix removes the contribution (3.4) from the seam of zero width. For compatibility with  $w = 0$ , we also require

$$\kappa_R(u, 0, \xi) = \kappa_R(u, \xi) \quad \Rightarrow \quad \kappa_0(u, \xi) = 1 \quad (3.14)$$

The boundary contribution is thus

$$\kappa_{\text{bdy}}(u, w, \xi) = \kappa_0(u) \kappa_R(u, w, \xi) = \kappa_0(u) \kappa_R(u, \xi) \kappa_w(u, \xi) \quad (3.15)$$

The remaining  $\mathcal{O}(1/N)$  contribution  $\ell(u)$  is different for each eigenvalue. It encodes the universal conformal properties of the model and can only be obtained by solving the full  $Y$ -system.

As a result of the factorization of the inversion identity (3.12), the non-universal quantities satisfy

$$\kappa_{\text{bulk}}(u)\kappa_{\text{bulk}}(u+\lambda) = \frac{\sin(\lambda+u)\sin(\lambda-u)}{\sin^2\lambda} \quad (3.16a)$$

$$\kappa_0(u)\kappa_0(u+\lambda) = \frac{\sin^2\lambda\sin(2\lambda+2u)\sin(2\lambda-2u)}{\sin^2 2\lambda\sin(\lambda+2u)\sin(\lambda-2u)} \quad (3.16b)$$

$$\kappa_R(u,\xi)\kappa_R(u+\lambda,\xi) = \Gamma(u)\Gamma(-u)/\Gamma(0)^2 \quad (3.16c)$$

$$\kappa_w(u,\xi)\kappa_w(u+\lambda,\xi) = \frac{\sin^2\xi_1\sin(\xi_{w+1}+u)\sin(\xi_{w+1}-u)}{\sin^2\xi_{w+1}\sin(\xi_1+u)\sin(\xi_1-u)}, \quad w > 0 \quad (3.16d)$$

together with the crossing symmetry  $\kappa(\lambda-u,\xi) = \kappa(u,\xi)$ . The last inversion relation is related to  $\kappa_\rho^{\text{PTC}}(u,\xi)$  and (3.21) of [28] by the trivial rescaling

$$\kappa_\rho^{\text{PTC}}(u,\xi) = \tilde{\kappa}_0(u,\xi)\kappa_w(u,\xi) = \frac{s(\xi+u)s(\xi_1-u)}{s(\xi)s(\xi_1)}\kappa_w(u,\xi), \quad \rho = w+1 \quad (3.17)$$

The  $\mathcal{O}(N)$  inversion relation for the bulk free energy  $f_{\text{bulk}}(u)$  has been solved by Baxter [58] using Fourier/Laplace transforms to give

$$-f_{\text{bulk}}(u) = \log \kappa_{\text{bulk}}(u) = \int_{-\infty}^{\infty} \frac{\cosh(\pi-2\lambda)t \sinh ut \sinh(\lambda-u)t}{t \sinh \pi t \cosh \lambda t} dt \quad (3.18)$$

The  $\mathcal{O}(1)$  inversion relation for the boundary free energy  $f_0(u)$  of the left Kac vacuum has been similarly solved in [28]

$$\begin{aligned} -f_0(u) = \log \kappa_0(u) &= \log \frac{\cos u \cos(\lambda-u)}{2 \cos \lambda \cos(u-\frac{\lambda}{2})} - \int_{-\infty}^{\infty} \frac{\sinh ut \sinh(\lambda-u)t}{t \sinh \pi t \cosh \lambda t} dt \\ &\quad - \int_{-\infty}^{\infty} \frac{\sinh \frac{\lambda t}{2} \sinh(\frac{3\lambda}{2}-\pi)t \cosh(\lambda-2u)t}{t \sinh \pi t \cosh \lambda t} dt, \quad 0 \leq \lambda \leq \pi \end{aligned} \quad (3.19)$$

Further modifications to the method lead to the derivation, given in Appendix B, of the new contribution  $f_R(u,\xi)$  arising from the Robin vacuum

$$-f_R(u,\xi) = \log \kappa_R(u,\xi) = \int_{-\infty}^{\infty} \frac{\sinh ut \sinh(\lambda-u)t}{t \sinh \pi t \cosh \lambda t} (\cosh \theta_{\xi+\lambda}t + \cosh \theta_{\xi+\alpha}t) dt \quad (3.20)$$

For  $x \in \mathbb{R}$ , the angle  $\theta_x \in [-\pi, \pi]$  is defined by

$$\theta_x + \pi = 2x \bmod 2\pi, \quad x \in \mathbb{R} \quad (3.21)$$

with jump discontinuities at  $x = k\pi$ ,  $k \in \mathbb{Z}$ . The function  $\theta_x$  is  $\pi$ -periodic in  $x$  on  $\mathbb{R}$ .

In accord with (3.7), the bulk and boundary energies of the Hamiltonian are obtained from these expressions by taking a derivative with respect to  $u$  and setting  $u = 0$

$$\mathcal{E}_{\text{bulk}} = -\sin \lambda \int_{-\infty}^{\infty} \frac{\tanh \lambda t \cosh(2\lambda-\pi)t}{\sinh \pi t} dt - \cos \lambda, \quad 0 < \lambda < \pi \quad (3.22a)$$

$$\mathcal{E}_0 = \sin \lambda \int_{-\infty}^{\infty} \frac{\tanh \lambda t \sinh(\frac{\pi}{2}-\frac{3\lambda}{2})t \sinh \frac{\lambda t}{2}}{\sinh \frac{\pi t}{2}} dt + \frac{1}{2 \cos \lambda}, \quad 0 < \lambda < \pi/2 \quad (3.22b)$$

$$\mathcal{E}_R(\xi,\alpha) = -\frac{1}{2} \sin \lambda \left[ \int_{-\infty}^{\infty} \frac{\tanh \lambda t}{\sinh \pi t} (\cosh \theta_{\xi+\lambda}t + \cosh \theta_{\xi+\alpha}t) dt + \cot(\xi+\lambda) - \cot(\xi+\alpha) \right] \quad (3.22c)$$

The Kac boundary energy  $\mathcal{E}_0$  exhibits a pole at  $\lambda = \frac{\pi}{2}$  and the integral formula requires an analytic continuation in  $\lambda$  performed in [28]

$$\mathcal{E}_0 = \frac{1}{2} + \frac{1}{2} \sin \lambda \int_{-\infty}^{\infty} [1 - 2 \sinh \frac{\lambda t}{2} \sinh (\frac{3\lambda}{2} - \pi)t] \frac{\tanh \lambda t}{\sinh \pi t} dt, \quad 0 < \lambda < \pi \quad (3.23)$$

The cotangents in the Robin boundary energy  $\mathcal{E}_R(\xi, \alpha)$  can be absorbed into the integral formula (3.22c) using

$$\cot x = - \int_{-\infty}^{\infty} \frac{\sinh \theta_x t}{\sinh \pi t} dt, \quad x \in \mathbb{R} \quad (3.24)$$

which yields

$$\mathcal{E}_R(\xi, \alpha) = \frac{1}{2} \sin \lambda \int_{-\infty}^{\infty} \frac{\sinh(\theta_{\xi+\lambda} - \lambda)t - \sinh(\theta_{\xi+\alpha} + \lambda)t}{\sinh \pi t \cosh \lambda t} dt, \quad 0 < \lambda < \pi \quad (3.25)$$

So far, we have only treated the case of the Robin vacuum. Note that there are no contributions to the boundary energies arising from the  $s$ -type seam. So, finally, we need to find the contribution from the  $r$ -type seam. In fact, this has been calculated in [28] but it is convenient to alternatively include this contribution with the contribution from the Robin vacuum. The expression for the Robin boundary energy (dressed by an  $r$ -type seam) is suggested as a consequence of an observation made in Appendix C. Namely, as an operator, the  $r$ -type Robin operator is algebraically equivalent (as a representation of the one-boundary TL algebra) to the vacuum Robin operator with the shifted parameters  $\xi_w = \xi + w\lambda$  and  $\alpha_{-w} = \alpha - w\lambda$ . The corresponding Hamiltonians are algebraically related in a similar manner. So it actually suffices to apply these shifts to the values of  $\xi$  and  $\alpha$  in (3.25) to obtain the  $(r, s)$  Robin boundary energies

$$\mathcal{E}_{\text{bdy}}(w, \xi) = \mathcal{E}_0 + \mathcal{E}_R(\xi) + \mathcal{E}_w(\xi) = \mathcal{E}_0 + \mathcal{E}_R(\xi_w, \alpha_{-w}), \quad \xi_w = \xi + w\lambda, \quad \alpha_{-w} = \alpha - w\lambda \quad (3.26)$$

A proper derivation of this formula, based on the inversion relations (3.16c) and (3.16d), is given in Appendix B. We have checked numerically that these shifted formulas agree with the expressions coming from [28]. Example plots of the analytic Robin boundary energies  $\mathcal{E}_{\text{bdy}}(w, \xi)$  against numerical values are shown in Figures 1 and 2. The analytic formulas for the boundary energies, including the jump discontinuities, are numerically confirmed with high accuracy.

## 4 Finite-Size Spectra

### 4.1 Finitized characters

We conjecture that, if  $\Delta_{r, s-\frac{1}{2}} \neq \Delta_{r', s'}$  for any  $r', s' \in \mathbb{N}$ , the  $(r, s-\frac{1}{2})$  Robin representations correspond to irreducible (highest weight) Virasoro Verma modules. If  $\Delta_{r, s-\frac{1}{2}} = \Delta_{r', s'}$  for some  $r', s' \in \mathbb{N}$ , the  $(r, s-\frac{1}{2})$  Robin representation may be reducible. These modules may exhibit Feigin-Fuchs structures [29]. In all cases, the associated conformal characters

$$\text{ch}_{\Delta}^{p, p'}(q) = q^{-\frac{c}{24} + \Delta} \widehat{\text{ch}}_{\Delta}^{p, p'}(q) = q^{-\frac{c}{24} + \Delta} \sum_E q^E \quad (4.1)$$

are the spectrum generating functions of the integer conformal energies  $E \geq 0$  with  $c = c^{p, p'}$  as in (1.1). The finitized characters, given by the finitized conformal partition functions in the  $(r, s)$  sector, are

$$\text{ch}_{r, s-\frac{1}{2}}^{p, p'; (N)}(q) = Z_{(1,1)|(r,s)}^{p, p'; (N)}(q) = q^{-\frac{c}{24} + \Delta_{r, s-\frac{1}{2}}^{p, p'}} \left[ \left[ \frac{N-d}{2} \right] + (-1)^{N-d-w} \left[ \frac{w}{2} \right] \right]_q, \quad r \in \mathbb{Z}, \quad s \in \mathbb{N} \quad (4.2)$$

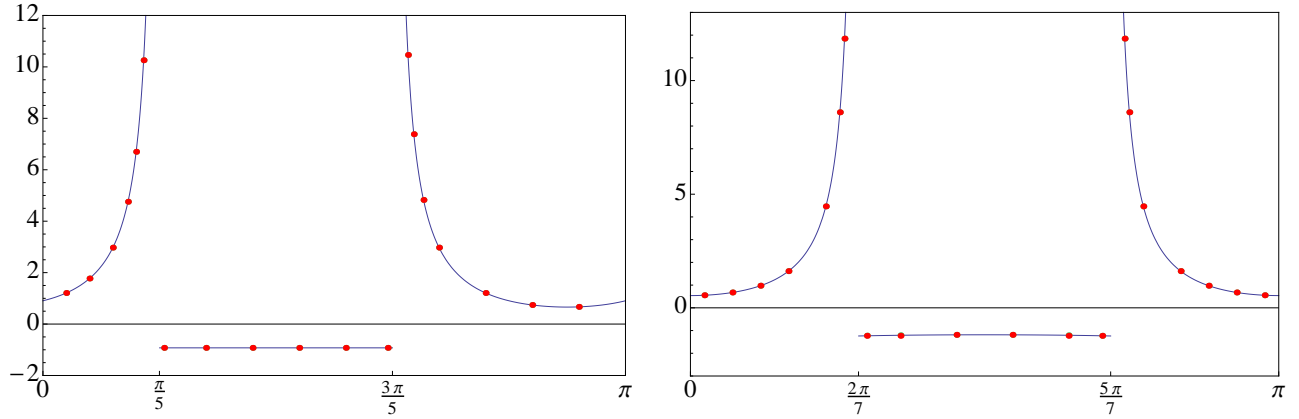


Figure 1: Plots of the boundary energy  $\mathcal{E}_{\text{bdy}}(w, \xi)$  against  $\xi$  for (i)  $\mathcal{LM}(2, 5)$  with  $\lambda = \frac{3\pi}{5}$ ,  $w = 3$  and (ii)  $\mathcal{LM}(4, 7)$  with  $\lambda = \frac{3\pi}{7}$ ,  $w = 2$ .

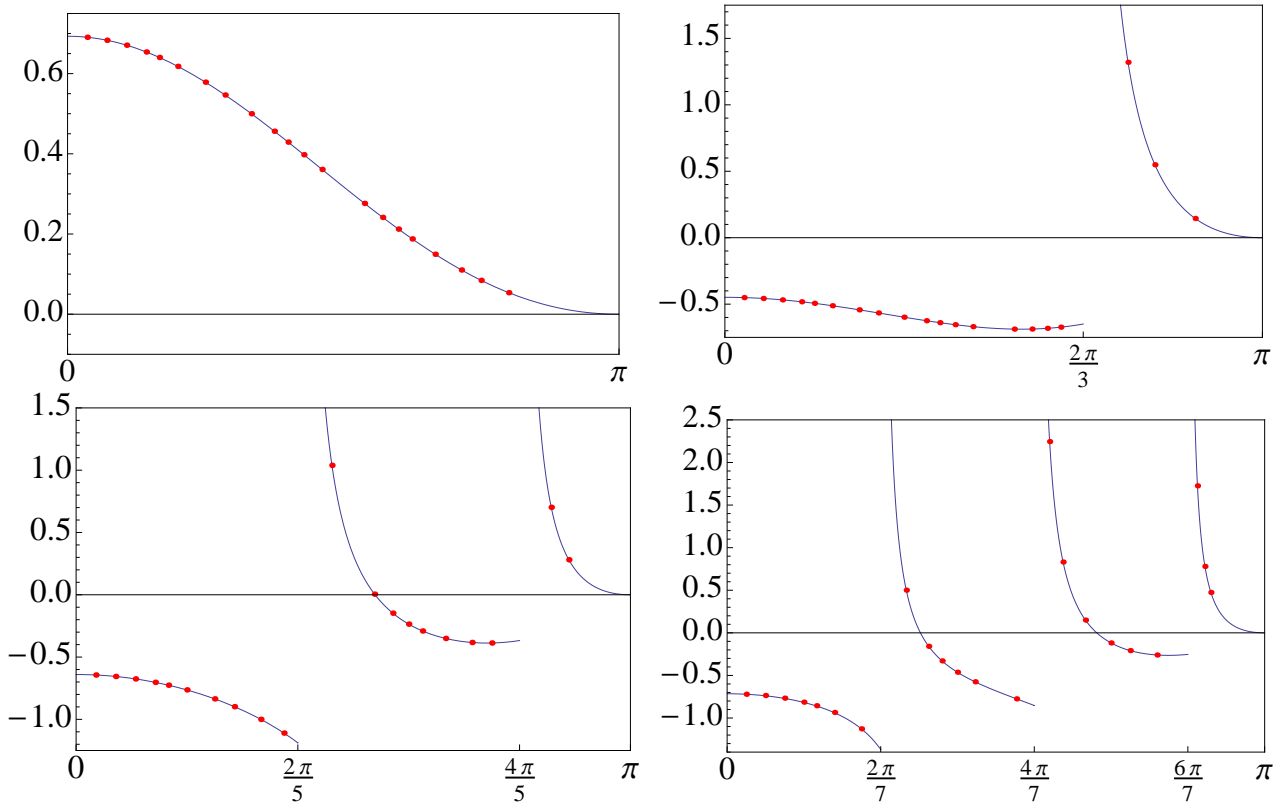


Figure 2: Plots of the boundary energy  $\mathcal{E}_{\text{bdy}}(w, \xi)$  against  $\lambda$  for  $\xi = -\frac{1}{2}\lambda$  with  $w = 0, 1, 2, 3$ .

$s$	$\ddots$	$\vdots$	$\vdots$	$\vdots$	$\vdots$	$\vdots$	$\vdots$	$\vdots$	$\vdots$	$\vdots$	$\vdots$	$\ddots$	
7	$\dots$	$\frac{261}{8}$	26	$\frac{161}{8}$	15	$\frac{85}{8}$	7	$\frac{33}{8}$	2	$\frac{5}{8}$	0	$\frac{1}{8}$	$\dots$
6	$\dots$	$\frac{225}{8}$	22	$\frac{133}{8}$	12	$\frac{65}{8}$	5	$\frac{21}{8}$	1	$\frac{1}{8}$	0	$\frac{5}{8}$	$\dots$
5	$\dots$	$\frac{575}{24}$	$\frac{55}{3}$	$\frac{323}{24}$	$\frac{28}{3}$	$\frac{143}{24}$	$\frac{10}{3}$	$\frac{35}{24}$	$\frac{1}{3}$	$-\frac{1}{24}$	$\frac{1}{3}$	$\frac{35}{24}$	$\dots$
4	$\dots$	$\frac{161}{8}$	15	$\frac{85}{8}$	7	$\frac{33}{8}$	2	$\frac{5}{8}$	0	$\frac{1}{8}$	1	$\frac{21}{8}$	$\dots$
3	$\dots$	$\frac{133}{8}$	12	$\frac{65}{8}$	5	$\frac{21}{8}$	1	$\frac{1}{8}$	0	$\frac{5}{8}$	2	$\frac{33}{8}$	$\dots$
2	$\dots$	$\frac{323}{24}$	$\frac{28}{3}$	$\frac{143}{24}$	$\frac{10}{3}$	$\frac{35}{24}$	$\frac{1}{3}$	$-\frac{1}{24}$	$\frac{1}{3}$	$\frac{35}{24}$	$\frac{10}{3}$	$\frac{143}{24}$	$\dots$
1	$\dots$	$\frac{85}{8}$	7	$\frac{33}{8}$	2	$\frac{5}{8}$	0	$\frac{1}{8}$	1	$\frac{21}{8}$	5	$\frac{65}{8}$	$\dots$
		-5	-4	-3	-2	-1	0	1	2	3	4	5	$r$

Figure 3: Robin Kac table of conformal weights  $\Delta_{r,s-\frac{1}{2}}$  for critical percolation  $\mathcal{LM}(2,3)$ .

$s$	$\ddots$	$\vdots$	$\vdots$	$\vdots$	$\vdots$	$\vdots$	$\vdots$	$\vdots$	$\vdots$	$\vdots$	$\vdots$	$\ddots$	
7	$\dots$	$\frac{287}{8}$	27	$\frac{155}{8}$	13	$\frac{63}{8}$	4	$\frac{11}{8}$	0	$-\frac{1}{8}$	1	$\frac{27}{8}$	$\dots$
6	$\dots$	$\frac{1287}{40}$	$\frac{119}{5}$	$\frac{667}{40}$	$\frac{54}{5}$	$\frac{247}{40}$	$\frac{14}{5}$	$\frac{27}{40}$	$-\frac{1}{5}$	$\frac{7}{40}$	$\frac{9}{5}$	$\frac{187}{40}$	$\dots$
5	$\dots$	$\frac{1147}{40}$	$\frac{104}{5}$	$\frac{567}{40}$	$\frac{44}{5}$	$\frac{187}{40}$	$\frac{9}{5}$	$\frac{7}{40}$	$-\frac{1}{5}$	$\frac{27}{40}$	$\frac{14}{5}$	$\frac{247}{40}$	$\dots$
4	$\dots$	$\frac{203}{8}$	18	$\frac{95}{8}$	7	$\frac{27}{8}$	1	$-\frac{1}{8}$	0	$\frac{11}{8}$	4	$\frac{63}{8}$	$\dots$
3	$\dots$	$\frac{891}{40}$	$\frac{77}{5}$	$\frac{391}{40}$	$\frac{27}{5}$	$\frac{91}{40}$	$\frac{2}{5}$	$-\frac{9}{40}$	$\frac{2}{5}$	$\frac{91}{40}$	$\frac{27}{5}$	$\frac{391}{40}$	$\dots$
2	$\dots$	$\frac{155}{8}$	13	$\frac{63}{8}$	4	$\frac{11}{8}$	0	$-\frac{1}{8}$	1	$\frac{27}{8}$	7	$\frac{95}{8}$	$\dots$
1	$\dots$	$\frac{667}{40}$	$\frac{54}{5}$	$\frac{247}{40}$	$\frac{14}{5}$	$\frac{27}{40}$	$-\frac{1}{5}$	$\frac{7}{40}$	$\frac{9}{5}$	$\frac{187}{40}$	$\frac{44}{5}$	$\frac{567}{40}$	$\dots$
		-5	-4	-3	-2	-1	0	1	2	3	4	5	$r$

Figure 4: Robin Kac table of conformal weights  $\Delta_{r,s-\frac{1}{2}}$  for the logarithmic Yang-Lee model  $\mathcal{LM}(2,5)$ .



These encode finitely truncated sets of the integer conformal energies of the infinite system. Setting  $q = 1$  in the  $q$ -binomial gives the correct counting of states (2.14). Taking the thermodynamic limit  $N \rightarrow \infty$  gives the Virasoro Verma characters

$$\text{ch}_{r,s-\frac{1}{2}}^{p,p'}(q) = \frac{q^{-\frac{c}{24} + \Delta_{r,s-\frac{1}{2}}^{p,p'}}}{(q)_\infty}, \quad r \in \mathbb{Z}, \quad s \in \mathbb{N}, \quad (q)_\infty = \prod_{n=1}^{\infty} (1 - q^n) \quad (4.3)$$

Example Robin Kac tables of conformal weights  $\Delta_{r,s-\frac{1}{2}}^{p,p'}$  are shown for  $\mathcal{LM}(2,3)$  and  $\mathcal{LM}(2,5)$  in Figures 3 and 4. These Kac tables can be extended to  $s \leq 0$  using the periodicity

$$\Delta_{r,s}^{p,p'} = \Delta_{r+p,s+p'}^{p,p'}, \quad (r,s) \equiv (r+p,s+p') \quad (4.4)$$

In the case that these conformal weights correspond to irreducible (highest weight) Virasoro Verma modules, any two modules with the same conformal weight are isomorphic and can be identified. As in the case of critical dense polymers  $\mathcal{LM}(1,2)$  [38], the Kac tables extended to  $s \leq 0$  are expected to encode the  $su(2)$  fusion rules.

## 4.2 Logarithmic limit

The conformal data and Kac characters of the Kac boundary conditions [17, 26–29] can be understood in terms of taking a logarithmic limit [60] of the conformal data of the rational nonunitary minimal models  $\mathcal{M}(m,m')$ . Symbolically, this limit of the minimal CFTs is given by

$$\lim_{m,m' \rightarrow \infty, \frac{m'}{m} \rightarrow \frac{p'}{p}+} \mathcal{M}(m,m') = \mathcal{LM}(p,p'), \quad 1 \leq p < p', \quad p, p' \text{ coprime} \quad (4.5)$$

The (one-sided) limit is taken through coprime pairs  $(m,m')$  with  $\frac{m'}{m} > \frac{p'}{p}$  to ensure the correct limiting ground states. The logarithmic limit is taken in the continuum scaling limit, after the thermodynamic limit. Since  $p \geq 1$ , the limit must ultimately be taken through a sequence of nonunitary models with  $m' - m > 1$ . The equality indicates the identification of the spectra of these CFTs. In principle, with  $(r,s)$  Robin boundary conditions on both sides of the strip, the Jordan cells appearing in the reducible yet indecomposable representations of the logarithmic minimal models should emerge in this limit but there are subtleties [60]. Here we consider the limit of chiral spectra, corresponding to a single character, for which purpose the logarithmic limit is robust in the sense that there are no Jordan cells and the limit is independent of the choice of the sequence.

Taking the logarithmic limit of the conformal data of the rational minimal models  $\mathcal{M}(m,m')$  yields the conformal data of the logarithmic minimal models  $\mathcal{LM}(p,p')$  including the central charges, conformal weights (1.1) and Kac characters

$$\chi_{r,s}^{p,p'}(q) = q^{-c/24 + \Delta_{r,s}^{p,p'}} \frac{(1 - q^{rs})}{(q)_\infty}, \quad r, s = 1, 2, 3, \dots \quad (4.6)$$

Explicitly, using  $|q| < 1$ , the limiting CFT data for  $r, s = 1, 2, 3, \dots$  are given by

$$c^{m,m'} = 1 - \frac{6(m' - m)^2}{mm'} \rightarrow 1 - \frac{6(p' - p)^2}{pp'} = c^{p,p'} \quad (4.7)$$

$$\Delta_{r,s}^{m,m'} = \frac{(rm' - sm)^2 - (m' - m)^2}{4mm'} \rightarrow \frac{(rp' - sp)^2 - (p' - p)^2}{4pp'} = \Delta_{r,s}^{p,p'} \quad (4.8)$$

$$\text{ch}_{r,s}^{m,m'}(q) = \frac{q^{-\frac{c}{24} + \Delta_{r,s}^{m,m'}}}{(q)_\infty} \sum_{k=-\infty}^{\infty} [q^{k(kmm' + rm' - sm)} - q^{(km+r)(km'+s)}] \rightarrow q^{-\frac{c}{24} + \Delta_{r,s}^{p,p'}} \frac{(1 - q^{rs})}{(q)_\infty} = \chi_{r,s}^{p,p'}(q) \quad (4.9)$$

The characters associated with half-integer Kac labels can also be obtained using the logarithmic limit. Since  $m$  and  $m'$  are coprime, at most one can be even. We fix these parities and take three different logarithmic limits. The half-integer boundary conditions, correspond to the logarithmic limit of free boundary conditions for the minimal models labelled [14] by either  $(r + \frac{m}{2}, s + \frac{m'-1}{2})$ ,  $(r + \frac{m-1}{2}, s + \frac{m'}{2})$  or  $(r + \frac{m-1}{2}, s + \frac{m'-1}{2})$  depending on the parities of  $m, m'$ . For  $m, m'$  large with  $r, s \in \mathbb{Z}$  finite, these sit at the center of a very large but finite rational Kac table. Explicitly, the three logarithmic limits give infinitely extended half-integer Kac tables with

$$\lim_{\substack{m, m' \rightarrow \infty, \\ m \text{ even}, m' \text{ odd}}} \frac{\text{ch}_{r + \frac{m}{2}, s + \frac{m'-1}{2}}^{m, m'}(q)}{\text{ch}_{r, s - \frac{1}{2}}^{p, p'}(q)} = \frac{q^{-\frac{c}{24} + \Delta_{r, s - \frac{1}{2}}^{p, p'}}}{(q)_\infty} = \text{ch}_{r, s - \frac{1}{2}}^{p, p'}(q), \quad r, s \in \mathbb{Z} \quad (4.10a)$$

$$\lim_{\substack{m, m' \rightarrow \infty, \\ m \text{ odd}, m' \text{ even}}} \frac{\text{ch}_{r + \frac{m-1}{2}, s + \frac{m'}{2}}^{m, m'}(q)}{\text{ch}_{r - \frac{1}{2}, s}^{p, p'}(q)} = \frac{q^{-\frac{c}{24} + \Delta_{r - \frac{1}{2}, s}^{p, p'}}}{(q)_\infty} = \text{ch}_{r - \frac{1}{2}, s}^{p, p'}(q), \quad r, s \in \mathbb{Z} \quad (4.10b)$$

$$\lim_{\substack{m, m' \rightarrow \infty, \\ m \text{ odd}, m' \text{ odd}}} \frac{\text{ch}_{r + \frac{m-1}{2}, s + \frac{m'-1}{2}}^{m, m'}(q)}{\text{ch}_{r - \frac{1}{2}, s - \frac{1}{2}}^{p, p'}(q)} = \frac{q^{-\frac{c}{24} + \Delta_{r - \frac{1}{2}, s - \frac{1}{2}}^{p, p'}}}{(q)_\infty} = \text{ch}_{r - \frac{1}{2}, s - \frac{1}{2}}^{p, p'}(q), \quad r, s \in \mathbb{Z} \quad (4.10c)$$

### 4.3 Finite-size corrections

Consider the  $\mathcal{LM}(p, p')$  lattice models on a strip with  $N$  columns and  $M$  double rows with Neumann boundary conditions applied on the left edge and  $(r, s)$  Robin boundary conditions on the right edge. The lattice partition function is

$$Z_{(1,1)|(r,s)}^{(N,M)} = \text{Tr} \mathbf{D}(u, \xi)^M = \sum_j D_j(u, \xi)^M = \sum_j e^{-ME_j(u, \xi)}, \quad j = 0, 1, 2, 3, \dots \quad (4.11)$$

where  $D_j(u, \xi)$  are the eigenvalues of  $\mathbf{D}(u, \xi)$  and  $E_j(u, \xi)$  are their associated energies. In the thermodynamic limit, only the ground state eigenvalue  $D_0(u, \xi)$  of the double row transfer matrix in each  $(r, s)$  sector contributes to the lattice partition function.

The conformal data of interest is accessible [7, 8] through the finite-size corrections to the eigenvalues of the transfer matrix or associated Hamiltonian. For the double row transfer matrix eigenvalues, the leading finite-size corrections for large  $N$  take the form

$$E_j = -\log D_j(u, \xi) = 2N f_{\text{bulk}}(u) + f_{\text{bdy}}(u, w, \xi) + \frac{2\pi \sin \vartheta}{N} \left( -\frac{c}{24} + \Delta_{r, s - \frac{1}{2}}^{p, p'} + k \right) + \dots, \quad k = 0, 1, 2, \dots \quad (4.12)$$

where  $k$  labels the level in the conformal tower. The anisotropy angle  $\vartheta$  [47] and modular nome  $q$  are

$$\vartheta = \frac{\pi u}{\lambda}, \quad \lambda = \frac{(p' - p)\pi}{p'}, \quad q = \exp\left(-2\pi \frac{M}{N} \sin \vartheta\right) \quad (4.13)$$

Referring to (1.1), the central charge of the CFT is  $c = c^{p, p'}$  while the spectrum of conformal weights is given by the possible values of  $\Delta_{r, s - \frac{1}{2}}^{p, p'}$  in the Kac table with excitations or descendants labelled by the non-negative integers  $k$ . Similarly, for the associated quantum Hamiltonian  $\mathcal{H}^{w, d}$ , the finite-size corrections of the eigenenergies take the form

$$E_j = N\mathcal{E}_{\text{bulk}} + \mathcal{E}_{\text{bdy}}(w, \xi) + \frac{\pi v_s}{N} \left( -\frac{c}{24} + \Delta_{r, s - \frac{1}{2}}^{p, p'} + k \right) + \dots, \quad k = 0, 1, 2, \dots \quad (4.14)$$

where  $v_s = \frac{\pi \sin \lambda}{\lambda}$  is the velocity of sound. The Hamiltonian energies  $\mathcal{E}_{\text{bulk}}$  and  $\mathcal{E}_{\text{bdy}}(w, \xi)$  are determined, up to the shift of the ground state energy, by evaluating the derivative at  $u = 0$  of  $f_{\text{bulk}}(u)$  and  $f_{\text{bdy}}(u, w, \xi)$  respectively.

#### 4.4 Numerical conformal weights

In this section, we present details of the numerical calculations for the conformal weights of the  $\mathcal{LM}(p, p')$  models with  $(r, s)$  Robin boundary conditions. Since it is numerically more efficient, we calculate the conformal spectra using the Hamiltonians rather than the double row transfer matrices. In Mathematica [61], it is convenient to represent a link state as an ordered list of the unique site connected to the  $N + w + d$  nodes numbered sequentially from left to right. The defects are folded, without introducing crossings, onto an  $s$ -type seam on the left. A node from which a boundary link emanates is considered connected to itself. For example, from (2.13),

$$\mathcal{V}_1^{(3,1)} = \text{span}\left\{\{2, 1, 3, 5|4\}\right\}, \quad \mathcal{V}_1^{(3,2)} = \text{span}\left\{\{2, 1, 6, 5|4, 3\}, \{6, 3, 2, 5|4, 1\}, \{6, 5, 4, 3|2, 1\}\right\} \quad (4.15)$$

The action of the TL generators on the vector space  $\mathcal{V}_d^{(N,w)}$  of link states is implemented succinctly in Mathematica using transformation rules. The matrix representatives are economically encoded as sparse matrices using dispatch tables. The additional generators in the Hamiltonian (3.8c) are similarly encoded directly as the matrix representatives of the operators mapping from  $\mathcal{V}_d^{(N,w)}$  to itself.

For a given sector, labelled by  $w, d$  or the quantum numbers  $(r, s)$ , the eigenvalues of the quantum Hamiltonian  $\mathcal{H}^{w,d}$  (3.8c) are obtained numerically using Mathematica for increasing system sizes  $N$  out to  $N + w + d \leq 26$ . For  $r = 0$ , the parity of  $N$  is not restricted. For  $r \neq 0$ , the parity of  $N$  is fixed by

$$\text{sgn}(r) = (-1)^{N+w+d} \quad (4.16)$$

Although the real transfer matrices are not symmetric, the transfer matrices in all sectors appear to be diagonalizable with real eigenvalues. Presumably, applying non-trivial boundary conditions on both the left and the right edge of the strip would lead to real but non-diagonalizable transfer matrices and reducible yet indecomposable representations. The first 10 to 20 dominant eigenvalues are obtained numerically using the Arnoldi method [62]. Estimates of the conformal eigenenergies  $E_j$ , and hence the conformal weights  $\Delta_{r,s-\frac{1}{2}}^{p,p'}$ , are extrapolated to infinite system size from the finite-size sequences (4.14) using a combination of Vanden Broeck-Schwartz [63] sequence acceleration and polynomial fits in  $1/N$ . There are no free parameters to fit and, since the bulk and boundary energies are known analytically, these extrapolation methods lead to accurate numerical results. The most accurate estimates occur for  $r = 0$  and  $s$  small for values of  $\lambda$  away from the endpoints at  $\lambda = 0, \pi$ . In such cases, the typical absolute error is of the order of  $10^{-7}$  with relative errors in the range  $10^{-8}$  to  $10^{-6}$ . Absolute and relative errors gradually increase to be of the order of  $10^{-1}$  for the plotted points with larger values of  $r, s$ . For larger seam widths, the errors increase and the accuracy decreases because, for given maximum total width, the maximum bulk width is decreased giving fewer data points for numerical extrapolation. Likewise, the accuracy decreases as  $\lambda$  approaches 0 or  $\pi$ .

Our numerical data is presented in a series of plots. Plots of the numerical conformal weights  $\Delta_{r,1/2}^{p,p'}$  as a function of  $\lambda$  for  $0 \leq r \leq 7$  and  $-1 \geq r \geq -7$  are shown in Figures 5 and 6. Plots of the numerical conformal weights  $\Delta_{r,3/2}^{p,p'}$  as a function of  $\lambda$  for  $0 \leq r \leq 6$  and  $-1 \geq r \geq -6$  are shown in Figures 7 and 8. Plots of the numerical conformal weights  $\Delta_{0,s-1/2}^{p,p'}$  for  $1 \leq s \leq 7$  are shown in Figure 9. Plots of the numerical conformal weights  $\Delta_{\pm 1,s-1/2}^{p,p'}$  and  $\Delta_{\pm 2,s-1/2}^{p,p'}$  as a function of  $\lambda$  are

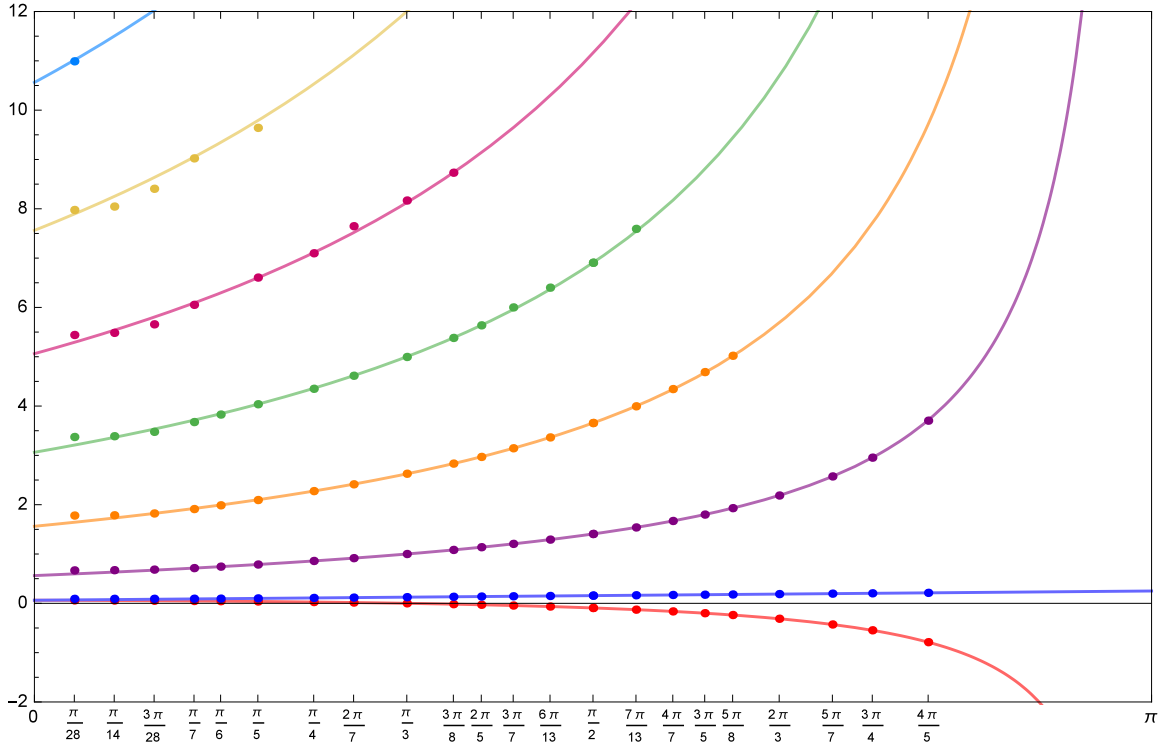


Figure 5: Plot of the numerical conformal weights  $\Delta_{r, \frac{1}{2}}^{p, p'}$  as a function of  $\lambda$  for  $r = 0, 1, 2, \dots, 6, 7$ .

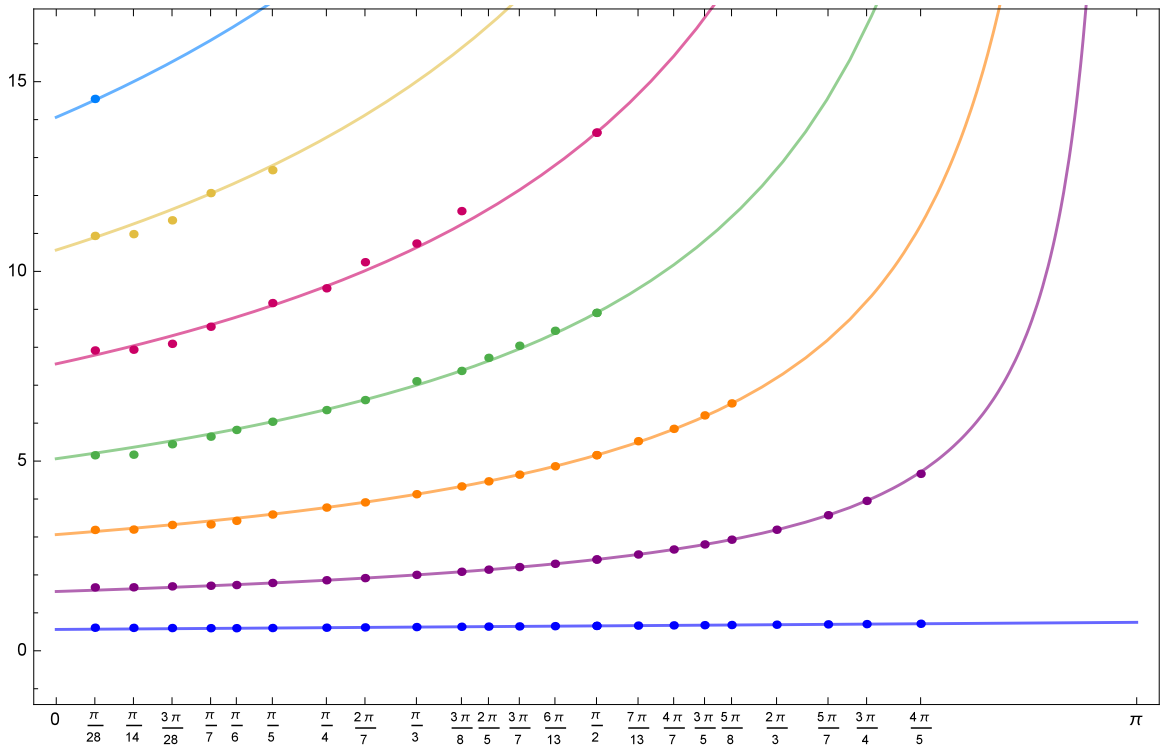


Figure 6: Plot of the numerical conformal weights  $\Delta_{r, \frac{1}{2}}^{p, p'}$  as a function of  $\lambda$  for  $r = -1, -2, \dots, -6, -7$ .

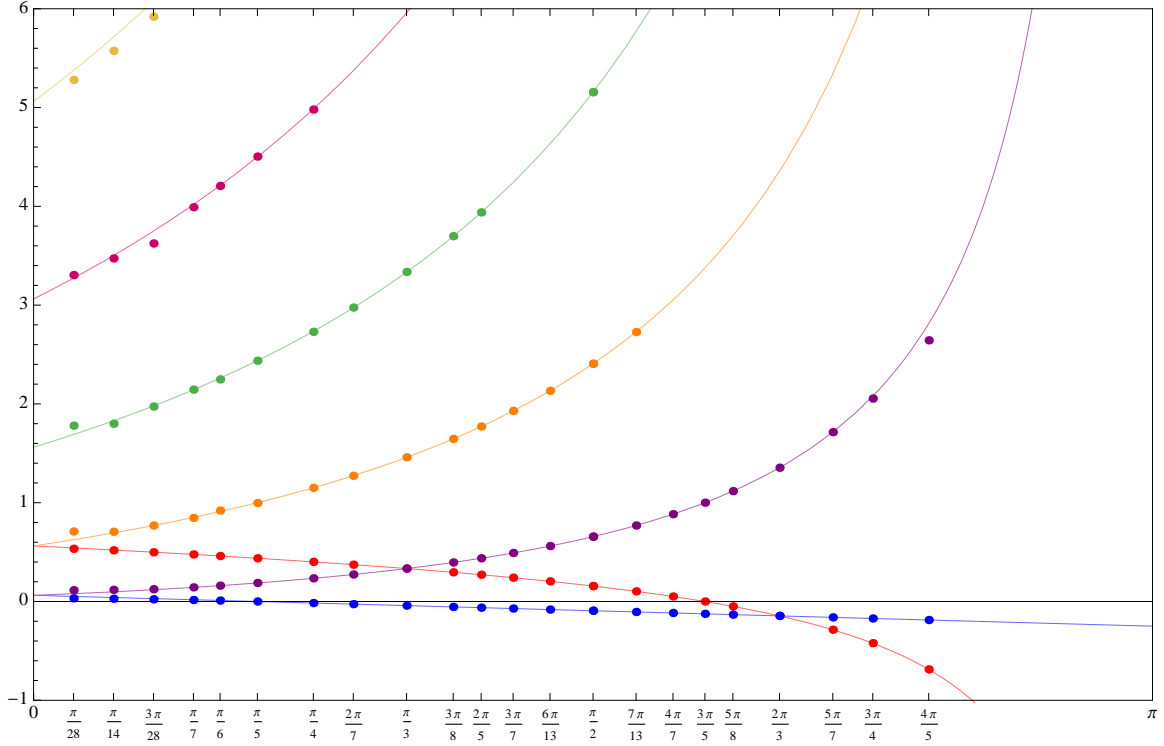


Figure 7: Plot of the numerical conformal weights  $\Delta_{r, \frac{3}{2}}^{p, p'}$  as a function of  $\lambda$  for  $r = 0, 1, 2, \dots, 5, 6$ .

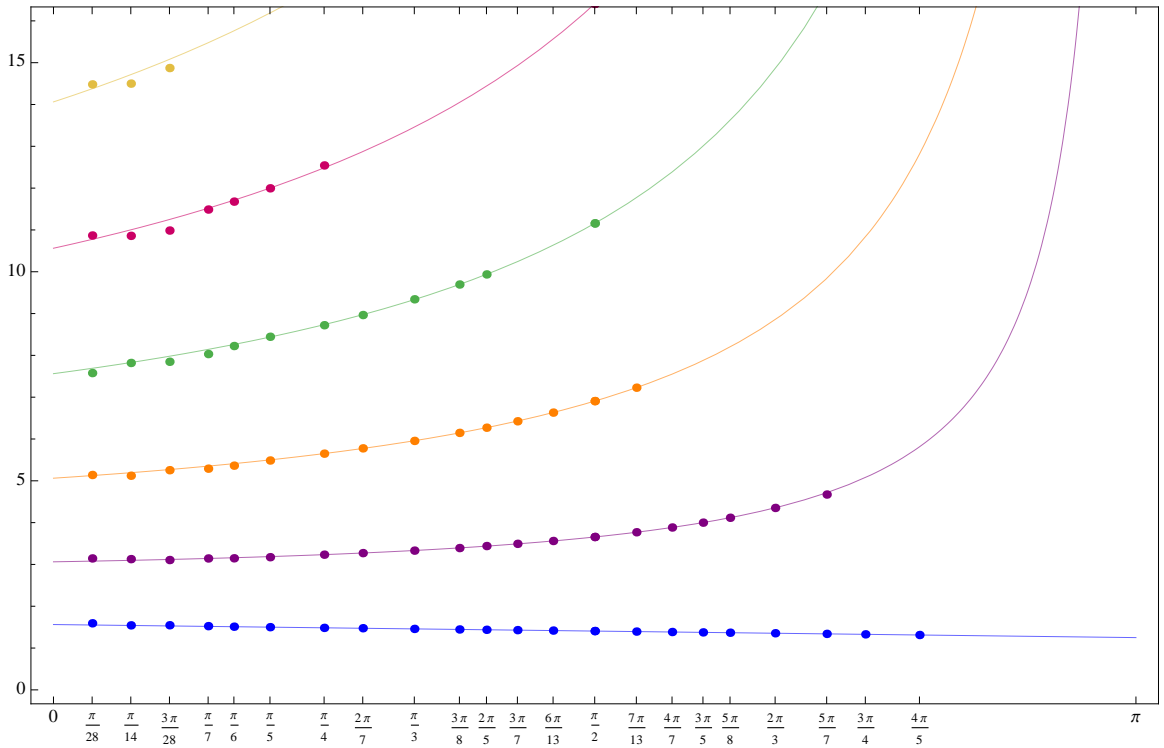


Figure 8: Plot of the numerical conformal weights  $\Delta_{r, \frac{3}{2}}^{p, p'}$  as a function of  $\lambda$  for  $r = -1, -2, \dots, -5, -6$ .

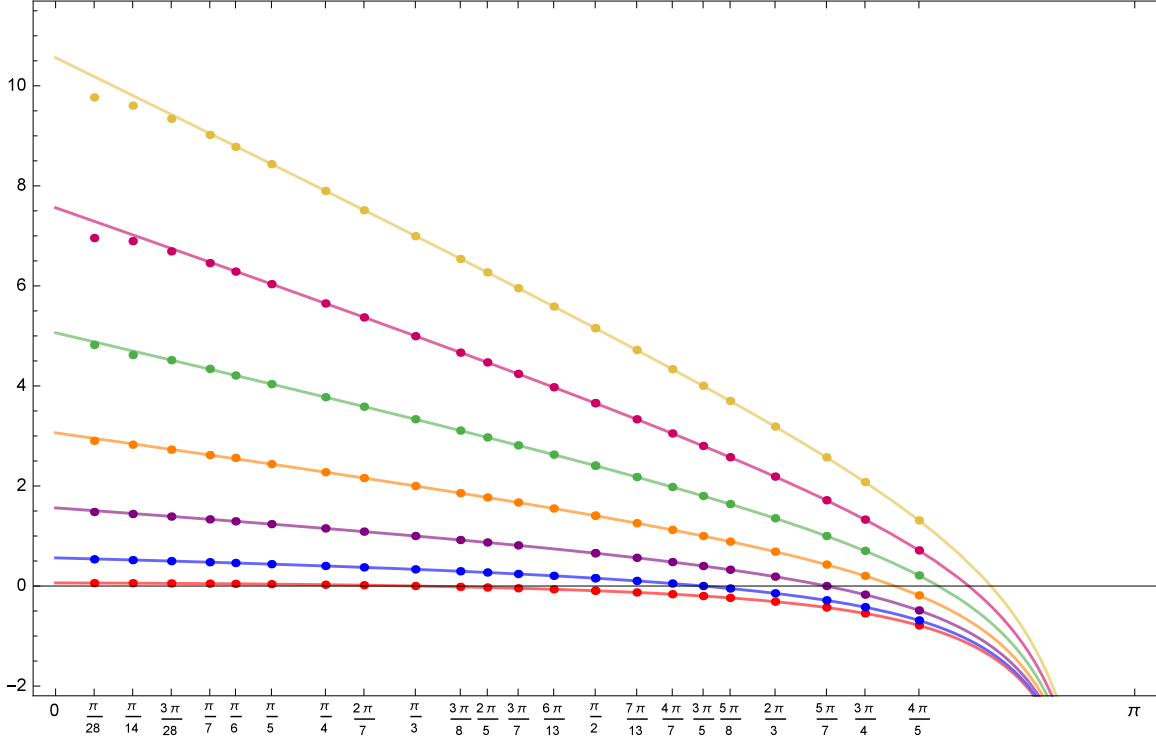


Figure 9: Plot of the numerical conformal weights  $\Delta_{0,s-\frac{1}{2}}^{p,p'}$  as a function of  $\lambda$  for  $s = 1, 2, \dots, 6, 7$ .

shown in Figures 10, 11, 12 and 13 respectively. The sequences of curves start with red, blue or blue, violet. The points in these plots at  $\lambda = \frac{\pi}{2}$ , related to critical dense polymers, are the values obtained analytically in [38].

#### 4.5 Numerical conformal partition functions

A consequence of the conjecture that the  $(r, s)$  Robin representations correspond to reducible or irreducible modules, with characters (4.3), is that the level degeneracies are determined by the partition numbers  $P_n$  [64] independent of the values of  $p, p', r$  and  $s$

$$\frac{1}{(q)_\infty} = \frac{1}{\prod_{n=1}^{\infty} (1 - q^n)} = \sum_{n=0}^{\infty} P_n q^n = 1 + q + 2q^2 + 3q^3 + 5q^4 + 7q^5 + 11q^6 + \dots \quad (4.17)$$

This expectation is well supported by the first 7-20 degeneracy levels obtained numerically. Typical results for  $\mathcal{LM}(3, 5)$  are

$$\widehat{\text{ch}}_{0, \frac{1}{2}}^{3,5}(q) = 1 + q + 2q^2 + 3q^3 + 5q^4 + 7q^5 + \dots \quad (4.18)$$

$$\widehat{\text{ch}}_{0, \frac{3}{2}}^{3,5}(q) = 1 + q + 2q^2 + 3q^3 + 5q^4 + \dots \quad (4.19)$$

$$\widehat{\text{ch}}_{2, \frac{1}{2}}^{3,5}(q) = 1 + q + 2q^2 + 3q^3 + 5q^4 + \dots \quad (4.20)$$

$$\widehat{\text{ch}}_{-2, \frac{1}{2}}^{3,5}(q) = 1 + q + 2q^2 + 3q^3 + \dots \quad (4.21)$$

$$\widehat{\text{ch}}_{2, \frac{3}{2}}^{3,5}(q) = 1 + q + 2q^2 + 3q^3 + \dots \quad (4.22)$$

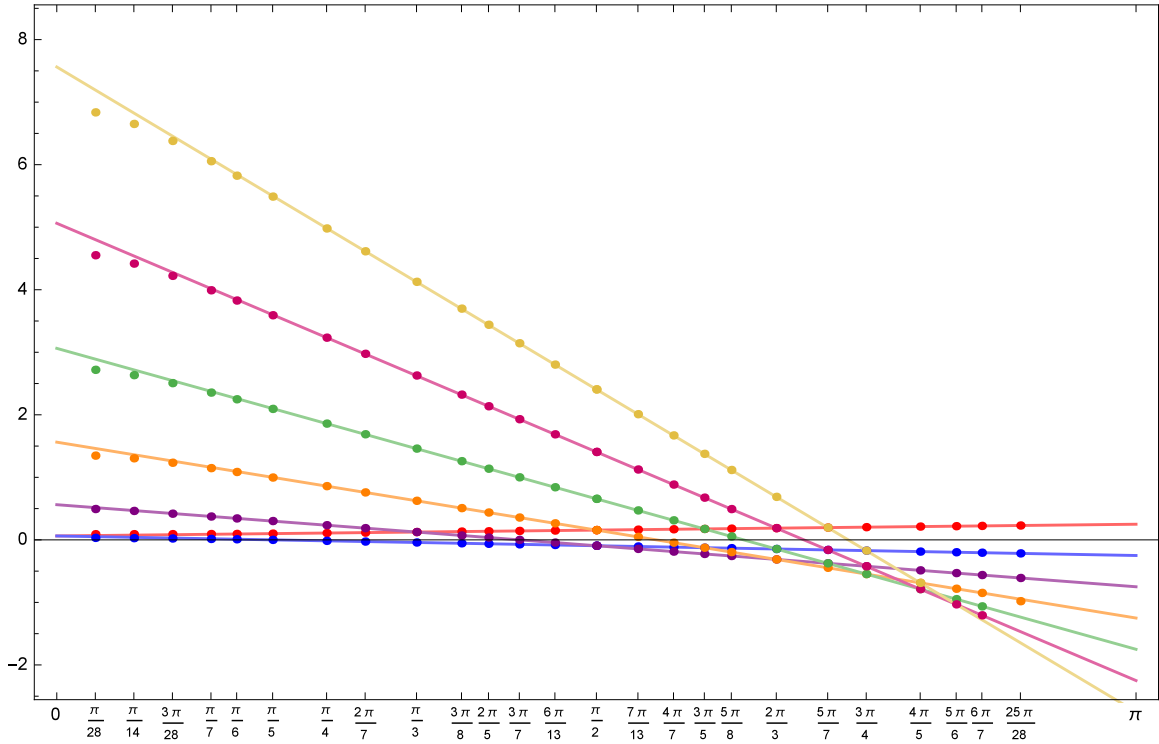


Figure 10: Plot of the numerical conformal weights  $\Delta_{1,s-\frac{1}{2}}^{p,p'}$  as a function of  $\lambda$  for  $s = 1, 2, \dots, 6, 7$ .

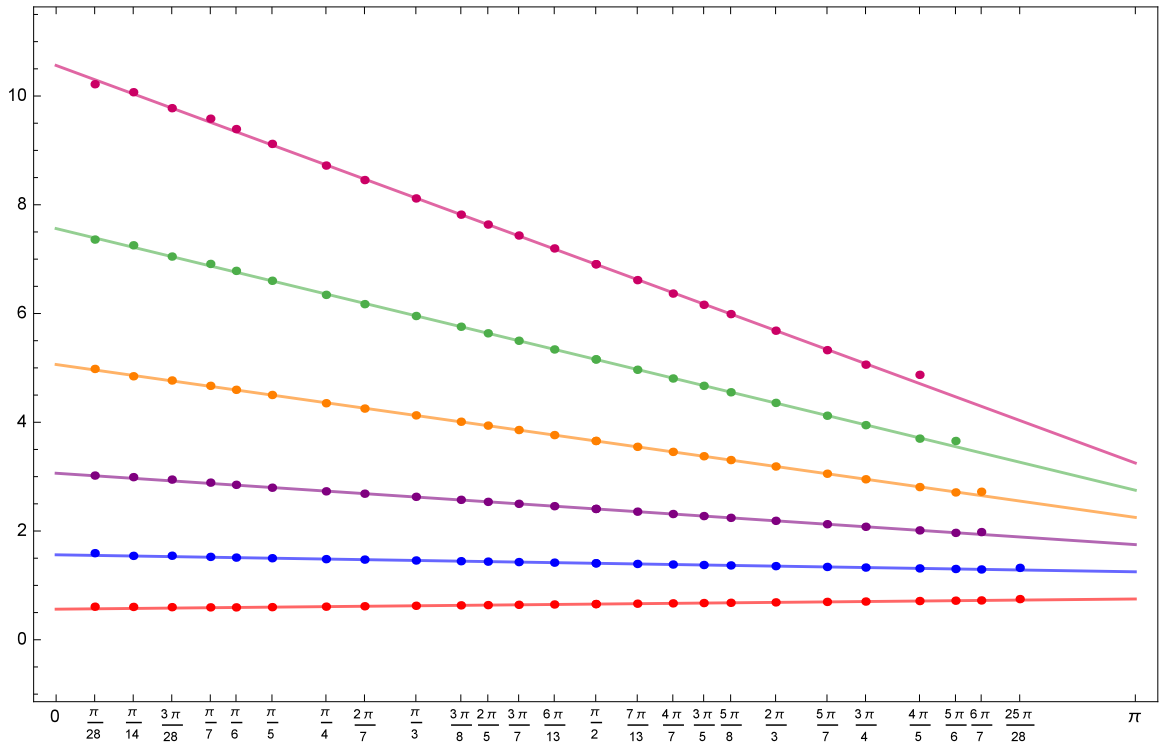


Figure 11: Plot of the numerical conformal weights  $\Delta_{-1,s-\frac{1}{2}}^{p,p'}$  as a function of  $\lambda$  for  $s = 1, 2, \dots, 6, 7$ .

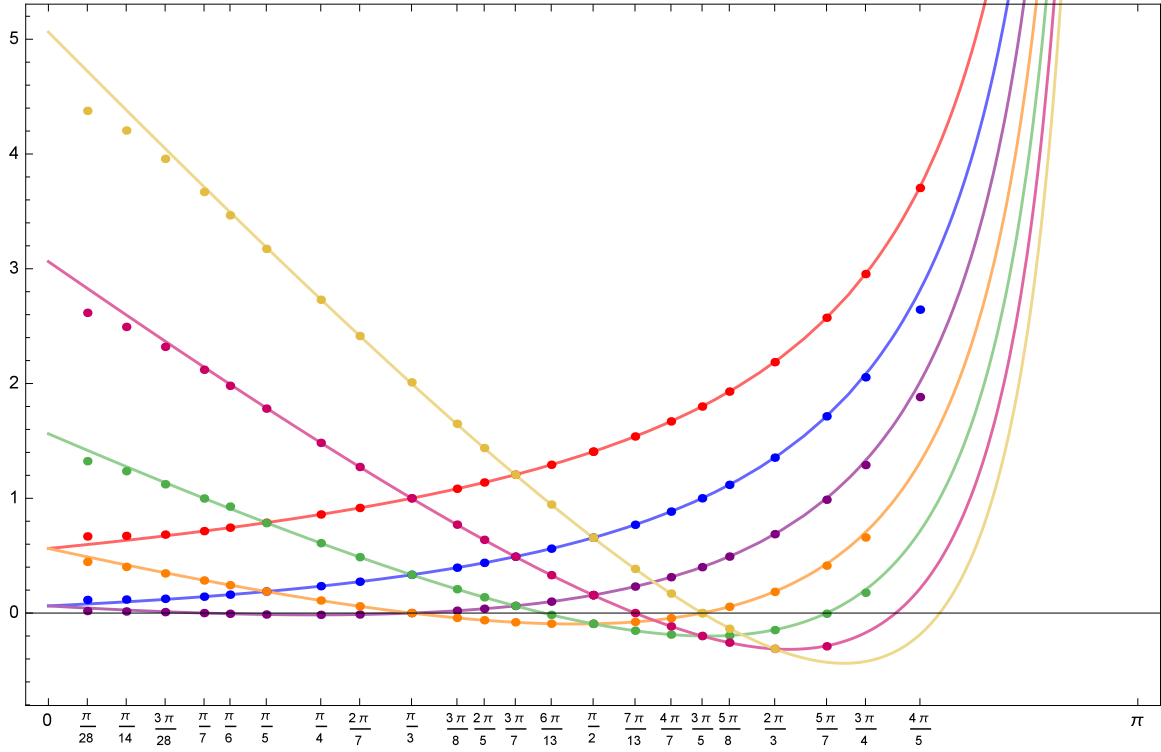


Figure 12: Plot of the numerical conformal weights  $\Delta_{2,s-\frac{1}{2}}^{p,p'}$  as a function of  $\lambda$  for  $s = 1, 2, \dots, 6, 7$ .

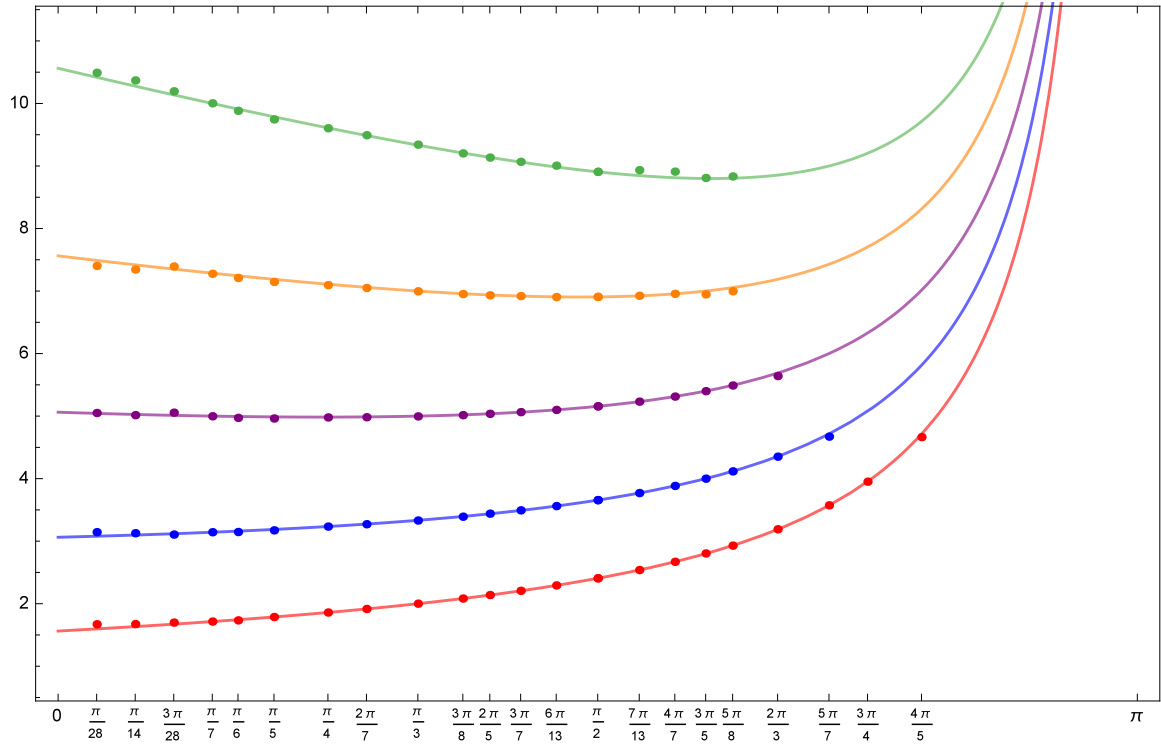


Figure 13: Plot of the numerical conformal weights  $\Delta_{-2,s-\frac{1}{2}}^{p,p'}$  as a function of  $\lambda$  for  $s = 1, 2, \dots, 6, 7$ .



$$\widehat{\text{ch}}_{-2, \frac{3}{2}}^{3,5}(q) = 1 + q + 2q^2 + 3q^3 + \dots \quad (4.23)$$

We have analyzed many other cases and the results for other logarithmic minimal models are similar.

## 5 Conclusion

In this paper, we have implemented the  $(r, s)$  Robin boundary conditions of Pearce, Rasmussen and Tipunin [38] for the general logarithmic minimal models  $\mathcal{LM}(p, p')$  [17] on the strip. The  $(r, s)$  boundary conditions are built from boundary  $r$ - and  $s$ -type seams of width  $w = \lfloor \frac{|r|p'}{p} \rfloor$  and  $d = s - 1$  columns respectively. This system is Yang-Baxter integrable in the presence of the boundary. We consider the commuting double row transfer matrices and the associated one-dimensional quantum chains which are described algebraically by the action of the one-boundary Temperley-Lieb algebra on suitable spaces of link states. The eigenvalues of the Hamiltonians are calculated numerically with Mathematica out to bulk system sizes  $N$  with  $N + w + d \leq 26$ . Estimates of the conformal weights in the various  $(r, s)$  Robin sectors are obtained numerically using finite-size corrections to the Hamiltonian eigenenergies. For  $r \neq 0$ , the extrapolated conformal weights depend on the parity of  $N$ . The results are neatly encoded by allowing  $r$  to be negative and fixing the parity of  $N$  by  $\text{sgn}(r) = (-1)^{N+w+d}$ . The bulk free energies are known and the boundary free energies are calculated analytically by solving the boundary inversion relations. Knowing the exact values of these non-universal quantities allows us to obtain accurate numerical estimates of the conformal weights which take the values  $\Delta_{r, s - \frac{1}{2}}^{p, p'}$ ,  $r \in \mathbb{Z}$ ,  $s \in \mathbb{N}$  where  $\Delta_{r, s}^{p, p'}$  is given by the usual Kac formula. The  $(r, s)$  Robin boundary conditions are thus conjugate to scaling operators with half-integer values for the Kac label  $s - \frac{1}{2}$ . Extensive numerical investigation of the level degeneracies support the conjecture that the characters of the associated reducible or irreducible modules are given by Virasoro Verma characters.

In this paper, we have implemented Robin boundary conditions on just one edge of the strip with the Kac vacuum boundary condition on the other edge leading to transfer matrices that are diagonalizable. It would be of interest to implement Robin boundary conditions on both edges of the strip in accord with Cardy fusion [40] on the lattice. This situation is described by the two-boundary Temperley-Lieb algebra [65, 66] and, in this case, the transfer matrices are expected to exhibit Jordan blocks and lead to reducible yet indecomposable representations of the Virasoro algebra. It would be interesting to know the complete closed set of fusion rules for these representations.

Lastly, there are strong indications [36] that there exist conformal weights for the logarithmic minimal models with half-integer values  $r - \frac{1}{2}$  for the first Kac label. It is an open question as to whether there are boundary conditions associated to these representations. But the application of the logarithmic limit (4.10) suggests that the associated boundary conditions cannot be far away.

## Acknowledgments

This work was initiated at the Asia Pacific Center for Theoretical Physics (APCTP). JEB acknowledges the Korea Ministry of Education, Science and Technology (MEST) for the support of the Young Scientist Training Program. He further thanks INFN for his post-doctoral fellowship within the grant GAST, which has also partially supported this project, together with the UniTo-SanPaolo research grant number TO-Call3-2012-0088 “*Modern Applications of String Theory*” (MAST), the ESF Network “*Holographic methods for strongly coupled systems*” (HoloGrav) (09-RNP-092 (PESC)) and the MPNS-COST Action MP1210. PAP thanks the APCTP for kind hospitality and the ICTP for support through a Visiting Scholar Award at APCTP. ET is supported by an Australian Postgraduate Award. We thank Jorgen Rasmussen and David Ridout for comments on the manuscript.

## A Derivation of the Inversion Relation

### A.1 Inversion relation for the Robin vacuum boundary

In this appendix, we derive the inversion relation (3.12) for the case  $w = 0$ . Diagrammatically, the product of the two transfer matrices on the left of the inversion identity (3.11) is

$$\frac{\beta^2 \Gamma(0)^2}{\tilde{\kappa}_0(u, \xi) \tilde{\kappa}_0(u + \lambda, \xi)} \mathbf{D}(u) \mathbf{D}(u + \lambda) = \text{Diagram} \quad (\text{A.1})$$

The first step is to insert, somewhere in the diagram, the identity

$$\text{Diagram} = \frac{1}{s_1(2u) s_1(-2u)} \text{Diagram} \quad (\text{A.2})$$

Using the Yang-Baxter equation, we push the inserted faces to either end

$$\frac{\beta^2 \Gamma(0)^2}{\tilde{\kappa}_0(u, \xi) \tilde{\kappa}_0(-u, \xi)} \mathbf{D}(u) \mathbf{D}(u + \lambda) = \frac{1}{s_1(2u) s_1(-2u)} \text{Diagram} \quad (\text{A.3})$$

To obtain the coefficient  $\phi(\lambda - u)\phi(\lambda + u)$ , we insert the identity decomposed into orthogonal projectors

$$I = \text{Diagram} = \frac{1}{\beta} \text{Diagram} + \frac{1}{\beta} \text{Diagram} \quad (\text{A.4})$$

The second term leads to the exponentially small second term on the right side of (3.11) which is neglected. The first term gives

$$\frac{\beta^2 \Gamma(0)^2}{\tilde{\kappa}_0(u, \xi) \tilde{\kappa}_0(-u, \xi)} \phi(\lambda - u) \phi(\lambda + u) = \frac{1}{\beta s_1(2u) s_1(-2u)} \text{Diagram} \quad (\text{A.5})$$

Using the identity

$$\begin{array}{|c|} \hline u+\lambda \\ \hline u \\ \hline \end{array} \begin{array}{c} \diagup \\ \diagdown \end{array} \lambda = s_1(u)s_1(-u) \begin{array}{|c|} \hline \text{---} \\ \hline \text{---} \\ \hline \end{array} \begin{array}{c} \diagup \\ \diagdown \end{array} = s_1(u)s_1(-u) \begin{array}{|c|} \hline \text{---} \\ \hline \text{---} \\ \hline \end{array} \begin{array}{c} \diagdown \\ \diagup \end{array} \quad (\text{A.6})$$

the projector can be pushed through to the left leaving only the identity behind. On the left boundary, the contribution is

$$\begin{array}{|c|} \hline \text{---} \\ \hline \text{---} \\ \hline \end{array} \begin{array}{c} \diagup \\ \diagdown \end{array} 2u \begin{array}{c} \diagdown \\ \diagup \end{array} \lambda = s_2(-2u) \begin{array}{|c|} \hline \text{---} \\ \hline \text{---} \\ \hline \end{array} \quad (\text{A.7})$$

where the boundary triangles have weight 1. We thus have

$$\frac{\phi(\lambda-u)\phi(\lambda+u)}{\tilde{\kappa}_0(u, \xi)\tilde{\kappa}_0(-u, \xi)} = \frac{[s_1(-u)s_1(u)]^N s_2(-2u)}{\beta^3 \Gamma(0)^2 s_1(2u)s_1(-2u)} \begin{array}{|c|} \hline -u & -u & \dots & -u \\ \hline \lambda-u & \lambda-u & \dots & \lambda-u \\ \hline \end{array} \begin{array}{c} \diagup \\ \diagdown \end{array} \begin{array}{c} u+\lambda \\ -2u \\ u \end{array} \quad (\text{A.8})$$

On the left, the Neumann boundary acts as a projector due to the drop-down (or push-through) property

$$\begin{array}{|c|} \hline u \\ \hline u+\lambda \\ \hline \end{array} \begin{array}{c} \diagdown \\ \diagup \end{array} = s_1(u)s_1(-u) \begin{array}{|c|} \hline \text{---} \\ \hline \text{---} \\ \hline \end{array} \begin{array}{c} \diagdown \\ \diagup \end{array} \quad (\text{A.9})$$

It can be pushed through to the right to give

$$\frac{\phi(\lambda-u)\phi(\lambda+u)}{\tilde{\kappa}_0(u, \xi)\tilde{\kappa}_0(-u, \xi)} = \frac{[s_1(u)s_1(-u)]^{2N} s_2(-2u)}{\beta^3 \Gamma(0)^2 s_1(2u)s_1(-2u)} \begin{array}{|c|} \hline \text{---} \\ \hline \text{---} \\ \hline \end{array} \begin{array}{c} \diagdown \\ \diagup \end{array} \begin{array}{c} u+\lambda \\ -2u \\ u \end{array} \quad (\text{A.10})$$

The remaining diagrammatic boundary term is evaluated by computing independently the eight configurations and summing over the results to give  $\beta s_2(2u)\Gamma(u)\Gamma(-u)$ . The relation thus simplifies to give the right side of (3.12) with  $w = 0$ .

## A.2 Inversion relation for a Robin boundary with an $r$ -type seam

The derivation of the inversion relation for an  $r$ -type Kac boundary seam is presented in Appendix C of [28]. The extension to the  $r$ -type Robin boundary seam presents no further difficulties. Setting

$$\mathcal{N} = \mathcal{N}^{(w)}(u, \xi)\mathcal{N}^{(w)}(u+\lambda, \xi) \quad (\text{A.11})$$

the first step is to insert two faces using the local inversion relation (A.2) and to push the two faces to the ends. No extra factors arise from the presence of the  $r$ -type seam

$$\mathcal{N}D(u)D(u+\lambda) = \frac{1}{s_1(2u)s_1(-2u)} \begin{array}{c} \begin{array}{c} \text{Diagram: A grid of blue squares with a vertical red dashed line (seam) in the middle. The grid is bounded by blue triangles on the left and right. The left triangle has a '2u' label. The right triangle has 'u+\lambda' and 'u' labels. The grid contains various parameters like -u, \lambda-u, \lambda+u, u, -u-\xi_w, \dots, -u-\xi_1, -u-\xi_0, u-\xi_0, u-\xi_w, u-\xi_1. Blue lines connect the squares to the triangles. Red arrows point to the seam.} \end{array} \end{array} \quad (\text{A.12})$$

Next, the second projector on the right side of (A.4) is inserted in the bottom two rows on the boundary between the seam and the bulk. The projector is pushed through the bottom rows of the bulk using (A.6), reflected at the boundary as in (A.7) and finally pushed back through the top rows of the bulk using (A.6) again

$$\mathcal{N}\phi(\lambda-u)\phi(\lambda+u) = \frac{[s_1(u)s_1(-u)]^{2N} s_2(-2u)}{\beta s_1(2u)s_1(-2u)} \times \begin{array}{c} \text{Diagram: Similar to (A.12), but with blue circles (projectors) on the top and bottom rows of the grid, between the seam and the right boundary.} \end{array} \quad (\text{A.13})$$

The results from [28] can be borrowed to push the projectors on the boundary through the  $r$ -type seam. The remaining boundary term corresponds to (A.10) so the final result is

$$\begin{aligned} \mathcal{N}\phi(\lambda+u)\phi(\lambda-u) &= [s_1(-u)s_1(u)]^{2N} \frac{s_2(-2u)s_2(2u)}{s_1(2u)s_1(-2u)} \Gamma(u)\Gamma(-u) \\ &\times \prod_{j=1}^w s_1(u+\xi_j)s_1(-u-\xi_j)s_1(u-\xi_j)s_1(-u+\xi_j) \end{aligned} \quad (\text{A.14})$$

The extra product is the contribution from the  $r$ -type seam which coincides with the same quantity computed in [28]. Using the identity

$$\frac{\prod_{j=1}^w s_1(u+\xi_j)s_1(-u-\xi_j)s_1(u-\xi_j)s_1(-u+\xi_j)}{\mathcal{N}^{(w)}(u,\xi)\mathcal{N}^{(w)}(u+\lambda,\xi)} = \frac{\sin(\xi+u)\sin(\xi-u)\sin(\xi_{w+1}+u)\sin(\xi_{w+1}-u)}{\beta^2 \Gamma(0)^2 \sin^2 \xi \sin^2 \xi_{w+1}} \quad (\text{A.15})$$

with  $\mathcal{N}^{(w)}(u,\xi)$  defined as in (3.3) this reduces to precisely (3.12).

## B Solution of the Inversion Relation

### B.1 Solution of the inversion relation for the Robin vacuum

Taking the logarithm of the inversion relations (3.16) gives functional equations that can be solved by Fourier/Laplace transforms. In this appendix, we solve (3.16c) for the Robin vacuum boundary free energy  $\kappa_R(u,\xi)$ . The right side of the inversion relation decomposes as

$$\frac{\Gamma(u)\Gamma(-u)}{\Gamma(0)^2} = \frac{\sin(\xi+\lambda+u)\sin(\xi+\lambda-u)}{\sin^2(\xi+\lambda)} \frac{\sin(\xi+\alpha+u)\sin(\xi+\alpha-u)}{\sin^2(\xi+\alpha)} \quad (\text{B.1})$$

As a result, the Robin vacuum boundary free energy is a sum of two contributions

$$-f_R(u, \xi) = \log \kappa_R(u, \xi) = g_{\xi+\lambda}(u) + g_{\xi+\alpha}(u) \quad (\text{B.2})$$

where the function  $g_x(u)$  is the solution of the fundamental inversion relation

$$g_x(u) + g_x(u + \lambda) = \log \frac{\sin(x+u)\sin(x-u)}{\sin^2 x}, \quad g_x(u) = g_x(\lambda - u) \quad (\text{B.3})$$

In this formulation, the problem is invariant under the translation of the variable  $x$  by a period  $\pi$ . It is also invariant under reversal of the sign of  $x$ . So, for simplicity, we can assume  $x > 0$ .

The general solution of the fundamental inversion relation takes the form

$$g_x(u) = \int_{-\infty}^{\infty} \frac{\sinh ut \sinh(\lambda - u)t \cosh(2x + k_x \pi)t}{t \sinh \pi t \cosh \lambda t} dt \quad (\text{B.4})$$

where the integer  $k_x \in \mathbb{Z}$  is chosen to ensure the convergence of the integral in the physical strip  $0 < \text{Re } u < \lambda$ . The integral converges if  $|2x + k_x \pi| < \pi$ , leading us to choose  $k_x$  such that  $\theta_x + \pi = 2x + (k_x + 1)\pi = 2x \pmod{2\pi}$ . As a consequence, the function  $g_x(u)$  is expressed in terms of the angle  $\theta_x$  with  $\theta_x + \pi = 2x \pmod{2\pi}$  as introduced in (3.21)

$$g_x(u) = \int_{-\infty}^{\infty} \frac{\sinh ut \sinh(\lambda - u)t \cosh \theta_x t}{t \sinh \pi t \cosh \lambda t} dt, \quad x \in \mathbb{R} \quad (\text{B.5})$$

This solution is  $\pi$ -periodic and even in the variable  $x$ . The result (3.20) for the boundary free energy  $f_R(u, \xi)$  is given by (B.2) with  $g_x(u)$  given by (B.5).

## B.2 Solution of the inversion relation with an $r$ -type seam

Referring to (3.13) and suppressing the dependence on  $\alpha$ , we have

$$\kappa_R(u, w, \xi) = \kappa_R(u, \xi) \kappa_w(u, \xi), \quad w > 0 \quad (\text{B.6})$$

From (3.12) and using

$$\Gamma(u) = \Gamma(u|\xi, \alpha) = \Gamma(u|\xi_w, \alpha_{-w}) \frac{s(\xi_1 - u)}{s(\xi_{w+1} - u)} \quad (\text{B.7})$$

the combined inversion relation is

$$\begin{aligned} \kappa_R(u, w, \xi) \kappa_R(u + \lambda, w, \xi) &= \frac{\Gamma(u)\Gamma(-u)}{\Gamma(0)^2} \frac{s(\xi_1)^2 s(\xi_{w+1} + u) s(\xi_{w+1} - u)}{s(\xi_{w+1})^2 s(\xi_1 + u) s(\xi_1 - u)} \\ &= \frac{\Gamma(u|\xi_w, \alpha_{-w}) \Gamma(-u|\xi_w, \alpha_{-w})}{\Gamma(0|\xi_w, \alpha_{-w})^2} \end{aligned} \quad (\text{B.8})$$

It follows that the inversion relation for  $w = 0$  is

$$\kappa_R(u, 0, \xi) \kappa_R(u + \lambda, 0, \xi) = \frac{\Gamma(u|\xi, \alpha) \Gamma(-u|\xi, \alpha)}{\Gamma(0|\xi, \alpha)^2} \quad (\text{B.9})$$

We conclude that  $\kappa(u, w, \xi)$  satisfies the same inversion relation as  $\kappa(u, 0, \xi)$  but with the replacements  $(\xi, \alpha) \mapsto (\xi_w, \alpha_{-w})$ . This is in accord with the algebraic equivalence, found in Appendix C.2, between the  $w = 0$  and  $w \geq 1$  Robin  $K$  matrices as representations of the one-boundary TL algebra.

## C Boundary Algebra

### C.1 Robin boundaries as representations of one-boundary TL algebra

In this section we show that, for  $\beta_1 = \beta_2 = 1$  and  $w \geq 0$ , the TL generators  $e_j$ ,  $j = 1, 2, \dots, N-1$  supplemented with the identity  $I$  and the Robin boundary generator

$$F_N(w) = \sum_{k=0}^w (-1)^k \frac{c_{2w-2k-1}}{c_1} e_N^{(k)}, \quad c_k = 2 \cos \frac{k\lambda}{2}, \quad e_N^{(k)} = e_N e_{N+1} \cdots e_{N+k}, \quad e_{N+w} = f_{N+w} \quad (\text{C.1})$$

form a representation of the one-boundary TL algebra (2.17) acting from the vector space  $\mathcal{V}_0^{(N,w)}$  to itself. It is then straightforward to allow for defects. The first few Robin boundary generators are

$$F_N(0) = f_N, \quad F_N(1) = e_N - e_N f_{N+1}, \quad F_N(2) = \frac{c_3}{c_1} e_N - e_N e_{N+1} + e_N e_{N+1} f_{N+2} \quad (\text{C.2})$$

Specifically, we show that

$$e_{N-1} F_N(w) e_{N-1} = B_1(w) e_{N-1}, \quad F_N(w)^2 = B_2(w) F_N(w) \quad (\text{C.3})$$

where

$$B_1(w) = \frac{c_{2w-1}}{c_1}, \quad B_2(w) = \frac{c_{2w+1}}{c_1} \quad (\text{C.4})$$

The first relation follows easily since, in expanding  $F_N(w)$  in  $e_{N-1} F_N(w) e_{N-1}$ , only the first term

$$\frac{c_{2w-1}}{c_1} e_{N-1} e_N e_{N-1} = \frac{c_{2w-1}}{c_1} e_{N-1} \quad (\text{C.5})$$

survives with  $e_N = f_N$  for  $w = 0$ . All of the other terms vanish since the  $e_{N-1}$  on the right can be pushed to the left until it sits immediately to the right of  $e_N$ . Using  $e_{N-1} e_N e_{N-1} = e_{N-1}$  leaves a word that starts with  $e_{N-1} e_{N+1}$  or  $e_{N-1} f_{N+1}$  and is killed because a half-arc occurs on the lower edge of the boundary seam between  $j = N+1$  and  $j = N+2$ .

Assuming  $w \geq 1$  and squaring the expanded  $F_N(w)$  gives

$$\begin{aligned} F_N(w)^2 &= \left[ \frac{c_{2w-1}}{c_1} e_N - \frac{c_{2w-3}}{c_1} e_N e_{N+1} \right]^2 + \frac{c_{2w-1}}{c_1} e_N \sum_{k=2}^w (-1)^k \frac{c_{2w-2k-1}}{c_1} e_N^{(k)} \\ &\quad - \frac{c_{2w-3}}{c_1} e_N e_{N+1} \sum_{k=2}^w (-1)^k \frac{c_{2w-2k-1}}{c_1} e_N^{(k)} \\ &= \frac{c_2 c_{2w-1} - c_{2w-3}}{c_1^2} \left[ c_{2w-1} e_N - c_{2w-3} e_N e_{N+1} + \sum_{k=2}^w (-1)^k c_{2w-2k-1} e_N^{(k)} \right] = \frac{c_{2w+1}}{c_1} F_N(w) \end{aligned} \quad (\text{C.6})$$

where we have used the TL algebra with  $e_N^2 = c_2 e_N$ . In the first step, we omitted all the terms that are killed because a half-arc occurs on the lower edge of the boundary seam. In the second step, we only use the TL algebra.

## C.2 Algebraic equivalence of Robin boundary conditions

In Appendix C.1, the parameter  $\alpha$  of the Robin boundary was fixed to enforce the equality  $\beta_1 = \beta_2 = 1$  of the boundary loop fugacities. However, useful relations can be derived by exploiting this extra degree of freedom. In this manner, the Robin boundary with an  $r$ -type seam of width  $w$  can be algebraically related to a vacuum ( $w = 0$ ) Robin boundary with shifted parameters  $\xi_w = \xi + w\lambda$ ,  $\alpha_{-w} = \alpha - w\lambda$ . This algebraic relation holds at the level of transfer matrices considered as elements of the (linear or planar) one-boundary TL algebra. Note that, since the two transfer matrices act on different spaces of link states, this relation cannot be used to deduce the conformal dimensions of the  $(r, s)$  Robin boundaries. On the other hand, the boundary energy is a common factor of the eigenvalues in every representation and is determined by algebraic relations. As such, it is constrained to satisfy the algebraic relation between Robin boundaries.

To show the algebraic equivalence of an  $r$ -type seam of width  $w \geq 1$  and parameters  $(\xi, \alpha)$  to a vacuum Robin boundary with parameters  $(\xi_w, \alpha_{-w}) = (\xi + w\lambda, \alpha - w\lambda)$  we consider the boundary  $K$  matrix as given in (5.12) of [38] and show that

$$= \sum_{k=0}^{w+1} \alpha_k^{(w)} e_N^{(k-1)} \cong \eta^{(w)}(u, \xi) \frac{s(\xi_1 - u)}{s(\xi_{w+1} - u)} \quad (\text{C.7})$$

where  $e_N^{(-1)} = I$ ,  $e_N^{(k)}$  is as in (C.1) and the  $\alpha$ -independent factor  $\eta^{(w)}(u, \xi)$  is given by (3.6). The symbol  $\cong$  indicates that the expressions are algebraically equivalent but act on different states. Setting  $\Gamma(u) = \Gamma(u|\xi, \alpha) = Rs(\xi_1 - u)s_0(\alpha + \xi + u)$ ,  $\beta_1 = Rs(\alpha)$ ,  $\beta_2 = Rs_{-1}(\alpha)$  and simplifying (5.12) of [38], the coefficients  $\alpha_k^{(w)}$  are given by

$$\frac{\alpha_k^{(w)}}{\eta^{(w)}(u, \xi)} = \begin{cases} \Gamma(u|\xi, \alpha) = \Gamma(u|\xi_w, \alpha_{-w}) \frac{s(\xi_1 - u)}{s(\xi_{w+1} - u)}, & k = 0 \\ (-1)^{k-1} Rs_{k-1-w}(\alpha) \frac{s(2u)s(\xi_1 - u)}{s(\xi_{w+1} - u)}, & k = 1, 2, \dots, w \\ (-1)^w \frac{s(2u)s(\xi_1 - u)}{s(\xi_{w+1} - u)}, & k = w + 1 \end{cases} \quad (\text{C.8})$$

It follows that

$$\frac{1}{\eta^{(w)}(u, \xi)} \sum_{k=0}^{w+1} \alpha_k^{(w)} e_N^{(k-1)} = \frac{s(\xi_1 - u)}{s(\xi_{w+1} - u)} [\Gamma(u|\xi_w, \alpha_{-w})I + s(2u)F_N(w)] \quad (\text{C.9})$$

where

$$F_N(w) = R \sum_{k=0}^{w-1} (-1)^k s_{k-w}(\alpha) e_N^{(k)} + (-1)^w e_N^{(w)} \quad (\text{C.10})$$

The TL generators  $e_j$ ,  $j = 1, 2, \dots, N-1$  supplemented with the identity  $I$  and the Robin boundary generator  $F_N(w)$  form a representation of the one-boundary TL algebra (2.17) acting from the vector space  $\mathcal{V}_0^{(N,w)}$  to itself. The first few Robin boundary generators are

$$\begin{aligned} F_N(0) &= f_N, & F_N(1) &= \beta_2 e_N - e_N f_{N+1}, & F_N(2) &= (\beta\beta_2 - \beta_1) e_N - \beta_2 e_N e_{N+1} + e_N e_{N+1} f_{N+2} \\ F_N(3) &= (\beta^2 \beta_2 - \beta_2 - \beta\beta_1) e_N - (\beta\beta_2 - \beta_1) e_N e_{N+1} + \beta_2 e_N e_{N+1} e_{N+2} - e_N e_{N+1} e_{N+2} f_{N+3} \end{aligned} \quad (\text{C.11})$$

In particular, following the arguments of Appendix C.1, it can be shown that

$$e_{N-1}F_N(w)e_{N-1} = B_1(w)e_{N-1}, \quad F_N(w)^2 = B_2(w)F_N(w) \quad (\text{C.12})$$

where

$$B_1(w) = Rs(\alpha_{-w}), \quad B_2(w) = Rs_{-1}(\alpha_{-w}) \quad (\text{C.13})$$

are related to the expressions for  $\beta_1, \beta_2$  by replacing  $\alpha$  with  $\alpha_{-w}$ . Indeed, setting  $\beta_1 = \beta_2 = 1$ , or equivalently  $R = 2 \sin \frac{\lambda}{2}$  and  $\alpha = \frac{\lambda + \pi}{2}$ , the results of this section reduce to those of Appendix C.1.

## References

- [1] A.A. Belavin, A.M. Polyakov, A.B. Zamolodchikov, *Infinite conformal symmetry in two-dimensional quantum field theory*, Nucl. Phys. **B241** (1984) 333–380.
- [2] D. Friedan, Z. Qiu and S. Shenker, *Conformal invariance, unitarity and critical exponents in two dimensions*, Phys. Rev. Lett. **52** (1984) 1575.
- [3] D.A. Huse, *Exact exponents for infinitely many new multicritical points*, Phys. Rev. **B30** (1984) 3908–3915.
- [4] G. Moore, N. Seiberg, *Classical and quantum conformal field theory*, Commun. Math. Phys. **123** (1989) 177–254.
- [5] P. Di Francesco, P. Mathieu and D. Sénéchal, *Conformal Field Theory*, Springer (1997).
- [6] R.E. Behrend, P.A. Pearce, V.B. Petkova, J.-B. Zuber, *On the classification of bulk and boundary conformal field theories*, Phys. Lett. **B444** (1998) 163–166; *Boundary conditions in rational conformal field theories*, Nucl. Phys. **B579** (2000) 707–773,
- [7] H.W.J. Blöte, J.L. Cardy, M.P. Nightingale, *Conformal invariance, the central charge, and universal finite-size amplitudes at criticality*, Phys. Rev. Lett. **56** (1986) 742–745.
- [8] I. Affleck, *Universal term in the free energy at a critical point and the conformal anomaly*, Phys. Rev. Lett. **56** (1986) 746–748.
- [9] R.J. Baxter, *Exactly solved models in statistical mechanics*, Academic Press, London, 1982.
- [10] G.E. Andrews, R.J. Baxter and P.J. Forrester, *Eight-vertex SOS model and generalised Rogers-Ramanujan-type identities*, J. Stat. Phys. **35** (1984) 193–266; P.J. Forrester and R.J. Baxter, *Further exact solutions of the eight-vertex SOS model and generalizations of the Rogers-Ramanujan identities*, J. Stat. Phys. **38** (1985) 435–472.
- [11] I.V. Cherednik, *Factorizing particles on a half-line and root systems*, Theor. Math. Phys. **61** (1984) 977–983.
- [12] E.K. Sklyanin, *Boundary conditions for integrable quantum systems*, J. Phys. **A21** (1988) 2375–2389.
- [13] R.E. Behrend, P.A. Pearce, D.L. O’Brien, *Interaction-round-a-face models with fixed boundary conditions: the ABF fusion hierarchy*, J. Stat. Phys. **84** (1996) 1–48.



- [14] R.E. Behrend, P.A. Pearce, *A construction of solutions to reflection equations for interaction-round-a-face models*, J. Phys. A **29** (1996) 7827–7835; *Integrable and conformal boundary conditions for  $\widehat{sl}(2)$  A-D-E lattice models and unitary minimal models*, J. Stat. Phys. **102** (2001) 577–640.
- [15] V. Pasquier, *Two-dimensional critical systems labelled by Dynkin diagrams*, Nucl. Phys. **B285** (1987) 162–172.
- [16] A. Cappelli, C. Itzykson, J. B. Zuber. *The A-D-E classification of minimal and  $A_1^{(1)}$  conformal invariant theories*, Comm. Math. Phys. **113** (1987) 1–26.
- [17] P.A. Pearce, J. Rasmussen, J.-B. Zuber, *Logarithmic minimal models*, J. Stat. Mech. (2006) P11017.
- [18] B.L. Feigin, A.M. Gainutdinov, A.M. Semikhatov, I. Yu. Tipunin, *Modular group representations and fusion in logarithmic conformal field theories and in the quantum group center*, Commun. Math. Phys. **265** (2006) 47–93.
- [19] P.A. Pearce, J. Rasmussen, *Solvable critical dense polymers*, J. Stat. Mech. (2007) P02015.
- [20] H.N.V. Temperley, E.H. Lieb, *Relations between the ‘percolation’ and ‘colouring’ problem and other graph-theoretical problems associated with regular planar lattices: Some exact results for the ‘percolation’ problem*, Proc. Roy. Soc. **A322** (1971) 251–280.
- [21] P. Goddard, A. Kent, D. Olive, *Virasoro algebras and coset space models*, Phys. Lett. **B152** (1985) 88–92.
- [22] P.A. Pearce, J. Rasmussen, *Coset graphs in bulk and boundary logarithmic minimal models*, Nucl. Phys. **B846** (2011) 616–649.
- [23] P.A. Pearce, J. Rasmussen, *Coset construction of logarithmic minimal models: branching rules and branching functions*, J. Phys. **A46** (2013) 355402.
- [24] A. Gainutdinov, D. Ridout, I. Runkel (Guest Editors), *Special issue on logarithmic conformal field theory*, J. Phys. A: Math. Theor. **46** (2013) Number 49.
- [25] V. Gurarie, *Logarithmic operators in conformal field theory*, Nucl. Phys. **B410** (1993) 535–549.
- [26] J. Rasmussen, *Classification of Kac representations in the logarithmic minimal models  $\mathcal{LM}(1, p)$* , Nucl. Phys. **B853** (2011) 404–435.
- [27] P.A. Pearce, J. Rasmussen, S. Villani, *Infinitely extended Kac table of solvable critical dense polymers*, J. Phys. A: Math. Theor. **46** (2013) 175202.
- [28] P.A. Pearce, E. Tartaglia, R. Couvreur, *Kac boundary conditions of the logarithmic minimal models*, J. Stat. Mech. (2014) P01018.
- [29] A.M. Morin-Duchesne, J. Rasmussen, D. Ridout, *Boundary algebras and Kac modules for logarithmic minimal models*, Nucl. Phys. **B899** (2015) 677–769.
- [30] H. Saleur, *New exact critical exponents for 2d self avoiding walks*, J. Phys. A: Math. Gen. **19** (1986) L807–L810.

- [31] B. Duplantier, *Exact critical exponents for two-dimensional dense polymers*, J. Phys. A: Math. Gen. **19** (1986) L1009–L1014.
- [32] H. Saleur, *Magnetic properties of the 2d  $n = 0$  vector model*, Phys. Rev. **B35** (1987) 3657–3660.
- [33] H. Saleur, *Conformal invariance for polymers and percolation*, J. Phys. A: Math. Gen. **20** (1987) 455–470.
- [34] D. Ridout, *On the percolation BCFT and the crossing probability of Watts*, Nucl. Phys. **B810** (2009) 503–526.
- [35] G Watts, *A Crossing Probability for Critical Percolation in Two-Dimensions*, J. Phys. A **29** (1996) L363–L368.
- [36] G. Delfino, *Parafermionic excitations and critical exponents of random cluster models and  $O(n)$  models*, Ann. Phys. **333** (2013) 1–11.
- [37] K. Gustafson, T. Abe, *(Victor) Gustave Robin: 1855–1897*, The Mathematical Intelligencer **20** (1998) 47–53; *The third boundary condition — was it Robin’s?* The Mathematical Intelligencer **20** (1998) 63–71.
- [38] P.A. Pearce, J.Rasmussen, I.Y. Tipunin, *Critical dense polymers with Robin boundary conditions, half-integer Kac labels and  $\mathbb{Z}_4$  fermions*, Nucl. Phys. **B889** (2014) 580–636.
- [39] J.L. Jacobsen, H. Saleur, *Conformal boundary loop models*, Nucl. Phys. **B788** (2008) 137–166.
- [40] J.L. Cardy, *Boundary conditions, fusion rules and the Verlinde formula*, Nucl. Phys. **B324** (1989) 581–596.
- [41] P.P. Martin, H. Saleur, *The blob algebra and the periodic Temperley-Lieb algebra*, Lett. Math. Phys. **30** (1994) 189–206.
- [42] P.P. Martin, D. Woodcock, *On the structure of the blob algebra*, J. Algebra **225** (2000) 957–988.
- [43] A. Nichols, V. Rittenberg, J. de Gier, *One-boundary Temperley-Lieb algebras in the XXZ and loop models*, J. Stat. Mech. (2005) P03003.
- [44] A. Nichols, *The Temperley-Lieb algebra and its generalizations in the Potts and XXZ models*, J. Stat. Mech. (2006) P01003.
- [45] A. Nichols, *Structure of the two-boundary XXZ model with non-diagonal boundary terms*, J. Stat. Mech. (2006) L02004.
- [46] V.F.R. Jones, *Planar algebras I*, arXiv:math.QA/9909027.
- [47] D. Kim, P.A. Pearce, *Scaling dimensions and conformal anomaly in anisotropic lattice spin models*, J. Phys. A: Math. Gen. **20** (1987) L451–L456.
- [48] A. Doikou and P. P. Martin, *Hecke algebraic approach to the reflection equation for spin chains*, J. Phys. A **36** (2003) 2203–2225.
- [49] P.A. Pearce, J. Rasmussen, E. Tartaglia, *Logarithmic superconformal minimal models*, J. Stat. Mech. (2014) P05001.

- [50] A.B. Zamolodchikov, *On the thermodynamic Bethe ansatz equations for reflection less ADE scattering theories*, Phys. Lett. **B253** (1991) 391–394; *Thermodynamic Bethe ansatz for RSOS scattering theories*, Nucl. Phys. **B358** (1991) 497–523.
- [51] A. Klümper, P.A. Pearce, *Conformal weights of RSOS lattice models and their fusion hierarchies*, Physica A **183** (1992) 304–350.
- [52] A. Kuniba, T. Nakanishi, J. Suzuki, *Functional relations in solvable lattice models I: Functional relations and representation theory*, Int. J. Mod. Phys. **A9** (1994) 5215; *T-systems and Y-systems in integrable systems*, J. Phys. A: Math. Theor. **44** (2011) 103001.
- [53] A. Morin-Duchesne, P.A. Pearce, J. Rasmussen, *Fusion hierarchies, T-systems and Y-systems of logarithmic minimal models*, J. Stat. Mech. (2014) P05012.
- [54] C.H.O. Chui, C. Mercat, P.A. Pearce, *Integrable boundaries and universal TBA functional equations*, Prog. Math. Phys. **23** (2002) 391–413.
- [55] A. Klümper, P.A. Pearce, *Analytic calculation of scaling dimensions: Tricritical hard squares and critical hard hexagons*, J. Stat. Phys. **64** (1991) 13–76.
- [56] P.A. Pearce, *Transfer-matrix inversion identities for exactly solvable lattice spins*, Phys. Rev. Lett. **58** (1987) 1502–1504.
- [57] Y.G. Stroganov, *A new calculation method for partition functions in some lattice models*, Phys. Lett. **A74** (1979) 116–118.
- [58] R.J. Baxter, *The inversion relation method for some two-dimensional exactly solved models in lattice statistics*, J. Stat. Phys **28** (1982) 1–41.
- [59] D.L. O’Brien, P.A. Pearce, R.E. Behrend, *Surface free energies and surface critical behavior of the ABF models with fixed boundaries*, Statistical Models, Yang-Baxter Equation and Related Topics, Tianjin, China (1996); D.L. O’Brien, P.A. Pearce, *Surface free energies, interfacial tensions and correlation lengths of the ABF models*, J. Phys. A: Math. Gen. **30** (1997) 2353–2366.
- [60] J. Rasmussen, *Logarithmic limits of minimal models*, Nucl. Phys. **B701** (2004) 516–528; *Jordan cells in logarithmic limits of conformal field theory*, Int. J. Mod. Phys. **A22** (2007) 67–82.
- [61] Wolfram Research, *Mathematica Edition: Version 10.0*, Wolfram Research Inc., Champaign, Illinois (2015).
- [62] W.E. Arnoldi, *The principle of minimized iterations in the solution of the matrix eigenvalue problem*, Quarterly of Applied Mathematics **9** (1951) 17–29.
- [63] J.-M. Vanden Broeck, L.W. Schwartz, *A one-parameter family of sequence transformations*, SIAM J. on Math. Anal. **10** (1979) 658–666; C.J. Hamer, M.N. Barber, *Finite-lattice extrapolations for  $\mathbb{Z}_3$  and  $\mathbb{Z}_5$  models*, J. Phys. A: Math. Gen. **14** (1981) 2009–2025.
- [64] N.J.A. Sloane, *The On-Line Encyclopedia of Integer Sequences*, published electronically at <http://oeis.org>, Sequence A000041 (partition numbers).
- [65] J. de Gier, A. Nichols, *The two-boundary Temperley-Lieb algebra*, J. Algebra **321** (2009) 1132–1167.
- [66] J. Dubail, J.L. Jacobsen, H. Saleur, *Conformal two-boundary loop model on the annulus*, Nucl. Phys. **B813** (2009) 430–459.